Applied Energy 377 (2025) 124678

Contents lists available at ScienceDirect

Applied Energy

journal homepage: www.elsevier.com/locate/apenergy

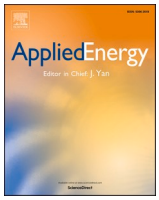

# A flexibility-oriented model for a sustainable local multi-carrier energy community: A hybrid multi-objective probabilistic-IGDT optimization approach

Sobhan Dorahaki [a,b], Mojgan MollahassaniPour [c], Masoud Rashidinejad [d], Pierluigi Siano [b,e], Miadreza Shafie-khah [f,g,*]

[a] Department of Electrical Engineering, Qatar University, Doha, 2713, Qatar
[b] Department of Management & Innovation Systems, University of Salerno, Fisciano, Italy
[c] Faculty of Electrical and Computer Engineering, University of Sistan and Baluchestan, Zahedan, Iran
[d] Department of Electrical Engineering, Shahid Bahonar University of Kerman, Kerman, Iran
[e] Department of Power Systems, National University of Science and Technology Politehnica Bucharest, Romania
[f] School of Technology and Innovations, University of Vaasa, 65200 Vaasa, Finland
[g] School of Engineering, RMIT University, Melbourne, VIC 3000, Australia

## HIGHLIGHTS

- Proposing a probabilistic approach for local multi-carrier energy systems operation.
- Developing a multi-objective model for cost and emissions of an energy community.
- Local multi-carrier energy systems model architecture with physical and managerial layers.
- Emphasizing the impact of flexibility and price on local multi-carrier energy systems performance.

## ARTICLE INFO

*Keywords:*
Energy community
Flexibility
Hydrogen fuel station
Hybrid probabilistic-IGDT approach
Local multi-carrier energy systems (LMCESs)
Power-to-gas (P2G)

## ABSTRACT

The Local Multi-Carrier Energy Systems (LMCESs) offer a great opportunity for Distributed Energy Resources (DERs) development in the energy system. The high variability of DERs output and the energy demands of the LMCESs increase the flexibility requirements in the upstream power system. In this context, an incentive-based mechanism needs to be considered by the power system operator to motivate the LMCESs to reduce the power exchange ramp rate with the upstream power system through an efficient energy management system in the LMCESs. This paper proposes a novel LMCESs optimization model that considers the flexibility constraint impacts on the economic and environmental objective functions. Additionally, the cost objective function accounts for the incentive to encourage cooperation from the LMCES in the flexibility program. To simultaneously address economic and emission-related objectives, the epsilon constraint method as a Multi-Criteria Decision-Making (MCDM) approach is employed. Moreover, a hybrid Probabilistic-IGDT method is employed to model the uncertainty of energy resources and demands. The optimization results underscore that increasing flexibility defaults while keeping flexibility prices constant reduces the operational cost of LMCES, but the impact on cost when increasing flexibility prices depends on whether the flexibility default is low or high. In particular, the flexibility price results in a cost reduction of 3.07 % in scenarios with low flexibility defaults and a significant reduction of 29.64 % in scenarios with high flexibility defaults.

* Corresponding Author.
*E-mail addresses:* sobhan.dorahaki@qu.edu.qa, Sobhandorahaki@gmail.com (S. Dorahaki), miadreza@gmail.com (M. Shafie-khah).

https://doi.org/10.1016/j.apenergy.2024.124678
Received 23 February 2024; Received in revised form 22 September 2024; Accepted 7 October 2024
Available online 15 October 2024

**Nomenclature**

*Acronyms*

| | |
|---|---|
| ADN | Active Distribution Networks |
| CHP | Combined Heat and Power |
| DERs | Distributed Energy Resources |
| DRPs | Demand Response Programs |
| ESS | Energy Storage Systems |
| CAES | Compressed Air Energy Storage |
| HVs | Hydrogen Vehicles |
| IGDT | Information Gap Decision Theory |
| kW | Kilowatt |
| LMCESs | Local Multi-Carrier Energy Systems |
| MCDM | Multi-Criteria Decision-Making |
| MILP | Mixed-Integer Linear Programming |
| P2G | Power-to-Gas |
| PDF | Probability Distribution Function |
| PV | Photovoltaic |
| RES | Renewable Energy Sources |
| TOPSIS | Technique for Order Preference by Similarity to Ideal Solution |

*Indices*

| | |
|---|---|
| $t, N_t$ | Index and set of times |
| $s, N_s$ | Index and set of scenarios |
| $v, N_v$ | Index and set of hydrogen vehicles |
| $i, j, N_i, N_j$ | Index and set of power nodes |
| $m, n, N_m, N_n$ | Index and set of gas nodes |
| $f, g, N_f, N_g$ | Index and set of heat nodes |
| $p, q, N_p, N_q$ | Index and set of water nodes |

*Parameters*

| | |
|---|---|
| $EL_{i,t,s}$ | Electrical demand before demand response (kW) |
| $\overline{F}^{G}, \underline{F}^{G}$ | Maximum and minimum gas flow (kW) |
| $\overline{F}^{EL}, \underline{F}^{EL}$ | Maximum and minimum electrical flow (kW) |
| $\overline{F}^{H}, \underline{F}^{H}$ | Maximum and minimum heat flow (kW) |
| $\overline{F}^{W}, \underline{F}^{W}$ | Maximum and minimum water flow ($m^3$) |
| $GL_{m,t,s}$ | Gas load (kW) |
| $HHV$ | High heat value (kW/$m^3$) |
| $\overline{H}^{B}, \underline{H}^{B}$ | Maximum and minimum heat of boiler unit (kW) |
| $H^{A,CHP}, H^{B,CHP}, H^{C,CHP}, H^{D,CHP}$ | Constant parameters of the output heat of CHP unit (kW) |
| $P^{A,CHP}, P^{B,CHP}, P^{C,CHP}, P^{D,CHP}$ | Constant parameters of the output power of CHP unit (kW) |
| $\overline{P}^{E,B}, \overline{P}^{E,S}$ | Maximum buying and selling power from/to the upstream network (kW) |
| $\overline{P}^{G}$ | Maximum buying gas from the upstream network (kW) |
| $\overline{P}^{GT}$ | Maximum power of microturbine unit (kW) |
| $\overline{P}^{H,B}, \overline{P}^{H,S}$ | Maximum buying and selling heat from/to the upstream network (kW) |
| $P^{PV}_{i,t,s}$ | Output power of PV system (kW) |
| $\overline{PE}^{ch,ES}, \overline{PE}^{dis,ES}$ | Maximum charging and discharging power of electrical storage (kW) |
| $\overline{PE}^{ch,TS}, \overline{PE}^{dis,TS}$ | Maximum charging and discharging heat of heat storage (kW) |
| $\overline{PH}^{ch,HTS}, \overline{PH}^{dis,HTS}$ | Maximum charging and discharging hydrogen of hydrogen storage ($m^3$) |
| $\overline{SOC}^{ES}, \underline{SOC}^{ES}$ | Maximum and minimum electrical storage capacity (kWh) |
| $\overline{SOC}^{HTS}, \underline{SOC}^{HTS}$ | Maximum and minimum hydrogen storage capacity ($m^3$) |
| $\overline{SOC}^{TS}, \underline{SOC}^{TS}$ | Maximum and minimum heat storage capacity (kWh) |
| $\overline{SOC}^{WS}$ | Maximum capacity of the water storage capacity ($m^3$) |
| $TL_{t,s}$ | Heat demand before demand response (kW) |
| $VT$ | Vehicle tank capacity ($m^3$) |
| $\overline{W}^{ch,WS}$ | Maximum input water of the water storage unit ($m^3$) |
| $\overline{W}^{dch,WS}$ | Maximum output water of the water storage unit ($m^3$) |
| $\overline{W}^{W,Des}$ | Maximum output water of the water desalination unit ($m^3$) |
| $\delta^{B}$ | Conversion rate efficiency of boiler unit |
| $\delta^{CHP}$ | Conversion rate efficiency of CHP unit |
| $\delta^{GT}$ | Conversion rate efficiency of microturbine unit |
| $\eta^{EF,W}$ | Efficiency rate of the water desalination unit |
| $\eta^{ES}$ | Electrical storage efficiency |
| $\eta^{P2G}$ | Power-to-Gas efficiency |
| $\eta^{TS}$ | Heat storage efficiency |
| $\vartheta^{E}, \vartheta^{T}$ | Participation rate of electrical and heat demands in demand response |
| $\zeta^{Def}$ | Default flexibility capacity (kW) |
| $\zeta$ | Cost division factor |
| $\pi^{E}_{t,s}$ | Electricity price ($/kW) |
| $\pi^{E,dn}$ | Electrical downward inconvenience incentive ($/kW) |
| $\pi^{E,up}$ | Electrical upward inconvenience incentive ($/kW) |
| $\pi^{Flex}$ | Flexibility incentive ($/kW) |
| $\pi^{G}_{t,s}$ | Gas price ($/kW) |
| $\pi^{H}_{t,s}$ | Heat price ($/kW) |
| $\pi^{T,dn}$ | Heat downward inconvenience incentive ($/kW) |
| $\pi^{T,up}$ | Heat upward inconvenience incentive ($/kW) |
| $\chi^{CO,Boiler}, \chi^{NO,Boiler}, \chi^{SO,Boiler}$ | CO, NO and SO emission coefficient of the boiler unit (kg/kW) |
| $\chi^{CO,CHP}, \chi^{NO,CHP}, \chi^{SO,CHP}$ | CO, NO and SO emission coefficient of the CHP unit (kg/kW) |
| $\chi^{CO,G}, \chi^{NO,G}, \chi^{SO,G}$ | CO, NO and SO emission coefficient of the gas demand (kg/kW) |
| $\chi^{CO,MT}, \chi^{NO,MT}, \chi^{SO,MT}$ | CO, NO and SO emission coefficient of the microturbine unit (kg/kW) |
| $\chi^{CO,Net}, \chi^{NO,Net}, \chi^{SO,Net}$ | CO, NO and SO emission coefficient of the upstream power (kg/kW) |
| $\omega_s$ | Probability |
| $\varpi^{EF,W}$ | Conversion rate between seawater and freshwater |

*Variables*

| | |
|---|---|
| $Cost^{E}_{t,s}$ | Electrical cost ($) |
| $Cost^{H}_{t,s}$ | Heat cost ($) |
| $Cost^{G}_{t,s}$ | Gas cost ($) |
| $Cost^{Flex}_{t,s}$ | Flexibility cost ($) |
| $Cost^{EDR}_{t,s}$ | Electrical demand response cost ($) |
| $Cost^{TDR}_{t,s}$ | Heat demand response cost ($) |
| $EL^{DR}_{t,s}$ | Electrical demand after demand response (kW) |
| $F^{G}_{m,n,t,s}, F^{El}_{i,j,t,s}, F^{H}_{f,g,t,s}, F^{W}_{p,q,t,s}$ | Gas, electrical, heat, and water energy flow (kW) |
| $GB^{B}_{m,t,s}$ | Gas consumption of boiler unit (kW) |
| $GC^{CHP}_{m,t,s}$ | Gas consumption of CHP unit (kW) |
| $GC^{GT}_{m,t,s}$ | Gas consumption of microturbine unit (kW) |
| $H^{B}_{f,t,s}$ | Output heat of boiler unit (kW) |
| $H^{CHP}_{f,t,s}$ | Output heat of CHP unit (kW) |
| $HG^{ch,HTS}_{s,t}, HG^{dis,HTS}_{s,t}$ | Charging and discharging of hydrogen storage unit ($m^3$) |
| $HG^{HV}_{s,v,t}$ | Consumption of hydrogen vehicles ($m^3$) |
| $HG^{P2G}_{s,t}$ | Output hydrogen of the P2G unit ($m^3$) |

| | |
|---|---|
| $I^{B}_{f,t,s}$ | Binary variable of boiler unit |
| $I^{CHP}_{i,t,s}$ | Binary variable of CHP unit |
| $I^{E,up}_{i,t,s}$, $I^{E,dn}_{i,t,s}$ | Binary variables of upward and downward electrical demand response |
| $I^{E}_{i,t,s}$, $I^{H}_{f,t,s}$ | Binary variables of electrical and heat energy exchange |
| $I^{ES}_{i,t,s}$ | Binary variable of the electrical storage unit |
| $I^{HTS}_{t,s}$ | Binary variable of the hydrogen storage unit |
| $I^{TS}_{f,t,s}$ | Binary variable of heat storage unit |
| $I^{T,up}_{f,t,s}$, $I^{T,dn}_{f,t,s}$ | Binary variables of upward and downward heat demand response |
| $I^{WS}_{p,t,s}$ | Binary variable of the water storage unit |
| $P^{CHP}_{i,t,s}$ | Output power of CHP unit (kW) |
| $P^{Des}_{i,t,s}$ | Power consumption of the water desalination unit (kW) |
| $P^{E,b}_{i,t,s}$, $P^{E,S}_{i,t,s}$ | Buying and selling power from/to the upstream network (kW) |
| $P^{G,b}_{m,t,s}$ | Buying gas from the upstream network (kW) |
| $P^{GT}_{i,t,s}$ | Output power of microturbine unit (kW) |
| $P^{H,b}_{f,t,s}$, $P^{H,S}_{f,t,s}$ | Buying and selling heat from/to the upstream network (kW) |
| $P^{P2G}_{i,s,t}$ | Electrical power consumption of P2G unit (kW) |
| $PE^{ch,ES}_{i,t,s}$, $PE^{dis,ES}_{i,t,s}$ | Charging and discharging power of electrical storage (kW) |
| $PE^{ch,TS}_{f,t,s}$, $PE^{dis,TS}_{f,t,s}$ | Charging and discharging heat of heat storage (kW) |
| $SOC^{ES}_{i,t,s}$ | Electrical storage level (kWh) |
| $SOC^{HTS}_{t,s}$ | Hydrogen storage level ($m^3$) |
| $SOC^{TS}_{f,t,s}$ | Heat storage level (kWh) |
| $SOC^{WS}_{p,t,s}$ | Water level of the water storage unit ($m^3$) |
| $TL^{DR}_{f,t,s}$ | Heat demands after demand response (kW) |
| $W^{ch,WS}_{p,t,s}$ | Input water to the water storage unit ($m^3$) |
| $W^{dch,WS}_{p,t,s}$ | Output water from the water storage unit ($m^3$) |
| $W^{SW}_{p,t,s}$ | Input seawater ($m^3$) |
| $W^{W,Des}_{p,t,s}$ | Output water of the desalination unit ($m^3$) |
| $\mu^{E,up}_{i,t,s}$, $\mu^{E,dn}_{i,t,s}$ | Upward and downward electrical demand response program (kW) |
| $\mu^{T,up}_{f,t,s}$, $\mu^{T,dn}_{f,t,s}$ | Upward and downward heat demand response program (kW) |
| $\zeta^{Flex}_{i,s,t}$ | The optimal flexibility (kW) |
| $\phi^{CHP}_{t,s}$ | Emission of CHP unit (kg) |
| $\phi^{Boiller}_{t,s}$ | Emission of boiler unit (kg) |
| $\phi^{G}_{t,s}$ | Emission of gas load (kg) |
| $\phi^{Net}_{t,s}$ | Emission of upstream power (kg) |
| $\phi^{MT}_{t,s}$ | Emission of microturbine unit (kg) |
| $\psi^{Emi}$ | Emission objective function (kg) |
| $\psi^{Cost}$ | Cost objective function ($) |

## 1. Introduction

### 1.1. Background and motivation

The global energy landscape is undergoing a transformative shift towards sustainability, driven by the need to mitigate climate change and reduce greenhouse gas emissions [1]. A key aspect of this transition is the increasing adoption of Distributed Energy Resources (DERs), such as Photovoltaic (PV) systems, wind turbines, Energy Storage Systems (ESSs), hydrogen fuel stations, and Power-to-Gas (P2G) units [2,3]. DERs offer a promising approach to decentralize energy generation, improve energy efficiency, and facilitate the integration of Renewable Energy Sources (RESs) into the grid. Local Multi-Carrier Energy Systems (LMCESs) have emerged as a propitious solution for enhancing the management of DERs within energy systems [4]. By integrating various energy carriers like electricity, heat, gas, and water, LMCESs provide a versatile platform to leverage the diverse capabilities of DERs and optimize the overall energy system performance [5,6]. However, the integration of DERs within LMCESs presents significant challenges in terms of system flexibility. The inherent variability in the output of renewable energy resources coupled with the dynamic nature of energy demands within LMCESs, can lead to rapid and unpredictable changes in the net load, imposing a significant challenge for the predominantly conventional thermal power plant-based upstream energy system [7]. Conventional power plants often struggle to quickly adjust their output to accommodate the rapid fluctuations in net load, impacting the overall flexibility and reliability of the power system [8]. To address this challenge, it is imperative for the upstream system operator to introduce a proactive flexibility program that incentivizes LMCES owners to actively manage the variability in power exchange with the upstream grid. This program should provide rewards or penalties based on the LMCES's level of engagement and performance in the flexibility initiative, encouraging them to adopt efficient energy management strategies and technological solutions to enhance system flexibility. Additionally, the risk attitudes of LMCES operators can significantly influence their energy scheduling decisions and their willingness to participate in the upstream flexibility program. Incorporating the risk preferences of LMCES operators into the optimization framework is indispensable to ensure the practical applicability and robustness of the solutions.

This paper addresses these challenges by developing a novel optimization model for a sustainable LMCES that incorporates a flexibility-oriented approach, a hybrid uncertainty modeling technique, and an incentive-based mechanism to encourage LMCES participation in the upstream flexibility program. The proposed framework aims to balance the economic and environmental objectives of the LMCES while accounting for the flexibility requirements of the upstream power system and the risk attitudes of the LMCES operator.

### 1.2. Literature review

LMCES have garnered significant attention for their potential to reduce environmental emissions and optimize system performance. Several studies have explored the integration of Demand Response Programs (DRPs) and ESSs to improve the flexibility and responsiveness of energy hub systems [9]. Additionally, research has focused on analyzing the effectiveness of active consumer participation in enhancing the resilience of LMCES [10]. Investigations into the potential of LMCES in reducing carbon emissions [11], as well as the development of optimal strategies for cost reduction through the implementation of DRPs [12], have been extensively examined. Furthermore, a multi-objective management framework has been devised to optimize the structure and performance of LMCES [13], while a non-linear stochastic optimization model has been proposed for multi-LMCES operations to minimize total operation costs [14]. The literature also highlights the substantial potential of LMCESs as adaptable platforms for integrating various energy generation and storage technologies [15], paving the way for more efficient and environmentally friendly energy utilization [16].

Besides the vital role of DERs in the power system, challenges such as high variability inherent in DERs output within LMCES have been underscored, posing threats to upstream grid stability [17] and flexibility [18]. In other words, flexibility in power systems has become

increasingly critical with the rise of RESs penetration rate in LMCES, which introduces variability and uncertainty into power grids [19]. Addressing these challenges through further research and innovation will be crucial for unlocking the full potential of LMCES systems and advancing sustainable energy systems. Several studies have explored various approaches to enhance upstream power system flexibility, focusing on DERs, demand side management, fast flexibility-driven generation, and advanced grid management techniques. For instance, [20] highlighted the role of DERs in providing flexibility at the interface between distribution and transmission systems. [21] explored the use of probabilistic solar power forecasts to inform the procurement of flexible ramp products in the California ISO. The utilization of ESSs and DRPs has been demonstrated to enhance system flexibility [18,22]; but it is accompanied by associated costs and user dissatisfaction [23]. However, ESSs and DRPs are widely addressed by researchers to address the flexibility challenges of the power system. For instance, [24] examined the role of DRP in enhancing the flexibility of transmission networks, particularly in scenarios involving wind farms, within the context of generation and transmission expansion planning. A model is presented in [25] to evaluate the flexibility of microgrids and power systems with the integration of flexibility tools such as DRP, ESSs, and electric vehicle parking lots. The study aims to maximize the profitability of these flexibility tools while minimizing energy costs and voltage deviation. The optimization problem is constrained by power flow equations, renewable generation limits, and the operational limits of the flexibility tools. [26,27] investigated the impact of ESSs technologies on power system flexibility but did not quantify the degree of flexibility within the systems. [28,29] assessed how short-term ESSs contribute to reducing carbon emissions, energy curtailment, and operating costs. However, these studies overlooked the effects of seasonal energy fluctuations, thereby not fully capturing the potential benefits of ESSs. [30] investigated the use of ESSs to boost distribution network flexibility, focusing on the optimal placement and sizing of ESSs to minimize investment costs while enhancing network flexibility. In [31], the economic feasibility of on-site ESSs for customers was analyzed, yet the flexibility index was not addressed. Additionally, flexibility evaluation indices for power systems across various time scales were defined in [32]. Similarly, [33] introduced a system flexibility balance index and evaluated the role of ESSs in supporting wind power integration. Nonetheless, these analyses did not take into account multi-energy complementary behavior, leaving some aspects of flexibility unexamined. [34] presented an imbalance mitigation strategy using flexible PV ancillary services, exemplified by a case study in Italy. By utilizing the flexibility of PV systems to provide ancillary services, such as reactive power support and voltage regulation, the study shows significant potential for reducing grid imbalances and enhancing the stability of power networks with high levels of PV penetration. Moreover, some paper address the role of flexible demand resources in participation in the flexibility improvement of power system. For instance, the value of demand-side flexibility is underscored by [35], who assess its impact on managing wind energy constraints and curtailment. By engaging flexible demand resources, such as industrial loads and electric vehicles, power systems can absorb excess wind generation during periods of high output and shift consumption to times of lower generation, thereby smoothing the variability of wind power and reducing the need for curtailment.

Furthermore, some papers in the literature focus on the flexibility market for flexibility resources. [36] describes a market model for Active Distribution Networks (ADN) that aims to generate financial returns from providing flexible services. In [37], the transactions between energy and flexibility are streamlined using a market-clearing model. This approach facilitates efficient coordination among various flexibility sources, simplifying the integration of flexibility into the energy market. The model aims to optimize the allocation of flexibility resources, ensuring that the supply and demand of both energy and flexibility services are balanced effectively, thereby enhancing the overall market efficiency and system stability. Additionally, [38] models the Flexibility Pricing Service (FPS) within an active distribution system that includes renewables and flexibility tools. In this work, a two-level optimization problem is formulated to maximize flexibility profits subject to specific constraints while determining the FPS. This necessitates the incorporation of flexibility requirements within the upstream power system, emphasizing the importance of incentive-based mechanisms to encourage cooperation from LMCESs in managing power exchange ramp rates [39]. Despite numerous research papers introducing the concept of the flexibility index and proposing solutions for enhancing power system flexibility, the pivotal role of the energy management system of LMCES in bolstering this flexibility has been largely overlooked in the literature. This highlights a notable research gap, emphasizing the need to incentivize LMCES participation in the flexibility program of the upstream energy network.

The uncertainty stemming from the inherent variability of renewable energy sources, dynamic energy demands, and prices is a critical aspect of effectively managing LMCESs. Stochastic programming approaches offer a promising avenue for tackling this challenge, but the escalating computational complexity associated with these methods necessitates the development of advanced optimization and control strategies to ensure the reliable and efficient operation of LMCESs. Previous studies have employed techniques such as the Information Gap Decision Theory (IGDT) and robust optimization to tackle forecast errors and uncertainties in energy system scheduling [40,41]. In a study by [40], a comprehensive risk hedging model was proposed to manage LMCES operations, aiming to minimize both energy procurement costs and financial risks. Meanwhile, [41] employed a robust optimization model to examine the interdependencies among various energy infrastructures, while considering their technical constraints and uncertainties associated with wind power. Further research has also been conducted on residential energy management, incorporating components like micro-Combined Heat and Power (CHP) units, plug-in hybrid electric vehicles, heat storage units, and rooftop solar panels, while accounting for uncertainties related to solar panel output using a two-point estimation method [42]. A novel approach to daily scheduling in smart grids has been presented, employing a smart LMCES framework and incorporating stochastic demand response mechanisms [43]. A probabilistic energy flow analysis framework for integrated electrical and gas systems has been proposed, investigating the coupling between gas-fired generators, electric-driven compressors, and energy hubs integrated with power-to-gas units [44]. Furthermore, [45] proposed a scenario-based generation and reduction algorithm to address the uncertain behavior of resources in the cooperative energy management approach for multi-LMCES.

Table 1 provides a comprehensive comparison of methods and tools from the literature, focusing on critical features such as the types of energy carriers involved, the application of multi-objective optimization, the integration of hydrogen, P2G technologies, and approaches to managing uncertainties. Similarly, Table 2 presents a detailed taxonomy of flexibility enhancement strategies within LMCES and broader power networks. It categorizes existing approaches across key dimensions, including flexibility constraints, incentive mechanisms, participation models, and resource integration. This taxonomy serves as a foundational reference for understanding the current landscape of flexibility strategies, emphasizing the potential role of LMCES in enhancing grid operations.

While substantial progress has been achieved in enhancing the flexibility and addressing uncertainty in LMCES, notable research gaps persist and need to be addressed. The focus should be on incentivizing LMCES participation in flexibility programs and developing robust optimization models to effectively manage uncertainties associated with renewable energy sources and demand dynamics. Hence, several research gaps are addressed in this paper as follows:

- ***Research gap #1:*** While there have been significant contributions to understanding flexibility in broader power systems, there is a lack of

**Table 1**
Comparison of methods and tools in the LMCES literature.

| Refs. | Energy Carriers | | | | Multi-Objective | Hydrogen Consideration | P2G | Uncertainty | Optimization Type |
|---|---|---|---|---|---|---|---|---|---|
| | E | W | G | H | | | | | |
| [2] | ✓ | × | ✓ | ✓ | ✓ | × | × | × | MINLP |
| [9] | ✓ | × | ✓ | ✓ | × | × | × | ✓ | MILP |
| [14] | ✓ | × | ✓ | ✓ | × | × | × | ✓ | MILP |
| [16] | ✓ | × | ✓ | ✓ | ✓ | ✓ | ✓ | ✓ | MINLP |
| [18] | ✓ | × | × | × | × | × | × | ✓ | MINLP |
| [19] | ✓ | × | × | × | × | × | × | × | MILP |
| [20] | ✓ | ✓ | ✓ | × | ✓ | × | ✓ | × | MILP |
| [21] | ✓ | × | × | × | ✓ | × | × | × | MINLP |
| [22] | ✓ | × | × | × | × | × | × | ✓ | MINLP |
| [24] | ✓ | × | × | × | × | × | × | × | MINLP |
| [25] | ✓ | × | × | × | ✓ | ✓ | ✓ | ✓ | MINLP |
| [26] | ✓ | ✓ | × | × | ✓ | × | × | ✓ | MILP |
| [27] | ✓ | × | ✓ | × | × | × | ✓ | × | MINLP |
| [28] | ✓ | × | × | × | × | × | × | × | MINLP |
| [29] | ✓ | × | × | × | ✓ | × | ✓ | × | MINLP |
| [30] | ✓ | × | × | × | ✓ | × | × | ✓ | MINLP |
| [31] | ✓ | × | × | × | × | × | × | × | MINLP |
| [32] | ✓ | × | × | × | ✓ | × | × | × | MILP |
| [33] | ✓ | ✓ | × | × | ✓ | ✓ | ✓ | × | MILP |
| [34] | ✓ | × | × | ✓ | ✓ | × | × | × | MILP |
| [35] | ✓ | × | ✓ | × | ✓ | × | × | ✓ | MILP |
| [36] | ✓ | × | × | × | ✓ | × | ✓ | × | MINLP |
| [38] | ✓ | × | × | × | ✓ | ✓ | × | ✓ | MILP |
| [39] | ✓ | × | ✓ | ✓ | ✓ | ✓ | × | × | MILP |
| [45] | ✓ | × | ✓ | ✓ | × | × | ✓ | ✓ | MILP |
| This Paper | ✓ | ✓ | ✓ | ✓ | ✓ | ✓ | ✓ | ✓ | MILP |
| **E: Electrical** | | | | **W: Water** | | **G: Gas** | | **H: Heat** | |

**Table 2**
Taxonomy of Flexibility Enhancement Strategies in LMCES and Power Networks.

| Refs. | Flexibility Constraint | Flexibility Incentive Mechanisms | LMCES Participation in Flexibility Programs | Risk Attitude Modeling of Operator in Flexibility Participation | Flexibility Resources |
|---|---|---|---|---|---|
| [18] | × | × | × | ✓ | DRP |
| [19] | × | × | × | × | ESS |
| [20] | × | ✓ | × | × | DERs |
| [21] | ✓ | ✓ | × | × | DERs |
| [22] | × | × | × | × | ESS |
| [24] | × | ✓ | × | × | Wind |
| [25] | ✓ | ✓ | ✓ | × | ESS + DRP |
| [26] | × | × | ✓ | × | ESS and DRP |
| [27] | ✓ | × | × | × | ESS |
| [28] | ✓ | × | × | × | ESS + CAES |
| [29] | × | × | ✓ | × | ESS |
| [30] | ✓ | × | × | ✓ | ESS |
| [31] | × | ✓ | × | × | ESS |
| [32] | ✓ | × | × | × | ESS + DRP |
| [33] | ✓ | × | × | × | Water Pumping + ESS |
| [34] | ✓ | × | × | × | ESS and DERs |
| [35] | ✓ | ✓ | ✓ | × | Demand-side Flexibility+ Heat Pumps |
| [36] | ✓ | × | × | × | DERs |
| [38] | ✓ | ✓ | ✓ | × | DRP |
| [39] | ✓ | × | ✓ | × | ESS + DRP |
| This paper | ✓ | ✓ | ✓ | ✓ | LMCES (e.g. DER + DRP + ESS) |

detailed examination on how LMCES can interact with grid operations through incentive-based mechanisms. Without a structured program for incentive-based flexibility, LMCES operators may have little motivation to participate. This lack of participation can limit the potential benefits that these systems could provide to the broader power grid, such as balancing supply and demand or mitigating grid congestion.

- ***Research gap #2:*** The literature generally acknowledges various approaches for modeling risk attitudes in energy systems. However, there is a research gap in applying these methods beyond flexibility improvement programs and evaluating the risk-averse and risk-seeking behaviors of LMCES operators. Specifically, existing studies have not sufficiently explored how the risk attitude of LMCES operators can impact their participation in flexibility programs, which is crucial for enhancing system reliability and operational efficiency.
- ***Research gap #3:*** Although elements such as P2G and hydrogen fuel stations have been considered within LMCES, there is a lack of comprehensive research on integrating all energy carriers (electrical, heat, gas, and water) within LMCES. There is a need for in-depth studies focusing on the integrated operation of P2G and hydrogen fuel stations, with specific attention to managing the synergies and challenges associated with multiple energy carriers in a unified framework.

These gaps present opportunities for further research and development in the field of LMCES.

### 1.3. Contribution

The paper proposes a flexibility-oriented hybrid multi-objective Probabilistic-IGDT model to address the operation cost and emission of the LMCES simultaneously using the epsilon constraint approach as a Multi-Criteria Decision-Making (MCDM) technique. This model incorporates electrical, water, gas, and heat energies, along with components such as the hydrogen fuel station, P2G Unit, CHP unit, heat and electrical storage units. The flexibility constraint imposed by the upstream entity is considered in the optimization problem to enhance the upstream flexibility of the energy system. The innovations presented in this paper effectively cater to the imperative need for enhancing flexibility, risk management, and realistic operation within the LMCES. The detailed elaborations are as follows:

- In order to address the first research gap an incentive-based mechanism within LMCES to enhance flexibility in the upstream network is proposed: By incentivizing flexibility in the trading patterns of LMCES, this approach, as a win-win strategy, has the potential to enhance the performance of the upstream energy system and bolster grid stability.
- To address the second shortcoming, the risk attitudes of LMCES owners into the hybrid multi-objective probabilistic-IGDT optimization approach is incorporated: By integrating the risk attitudes of LMCES owners into energy scheduling and trading processes through this approach, a more refined landscape is provided for determining the participation of the LMCES owner in the flexibility program. This incorporation enhances the decision-making process by taking into account the varying risk preferences of LMCES owners (risk-averse or risk-seeker), ultimately leading to more effective and tailored participation in energy scheduling and trading activities.
- In order to address the third research gap a LMCES comprising electrical, heat, gas, and water energy carriers, along with technologies like hydrogen fuel stations and P2G units is provided: The innovations introduced by hydrogen fuel stations and P2G units play a crucial role in supporting the flexibility constraint model, ensuring that the LMCES can dynamically respond to fluctuations in energy supply and demand. These enhancements collectively contribute to the development of more sustainable and resilient energy systems.

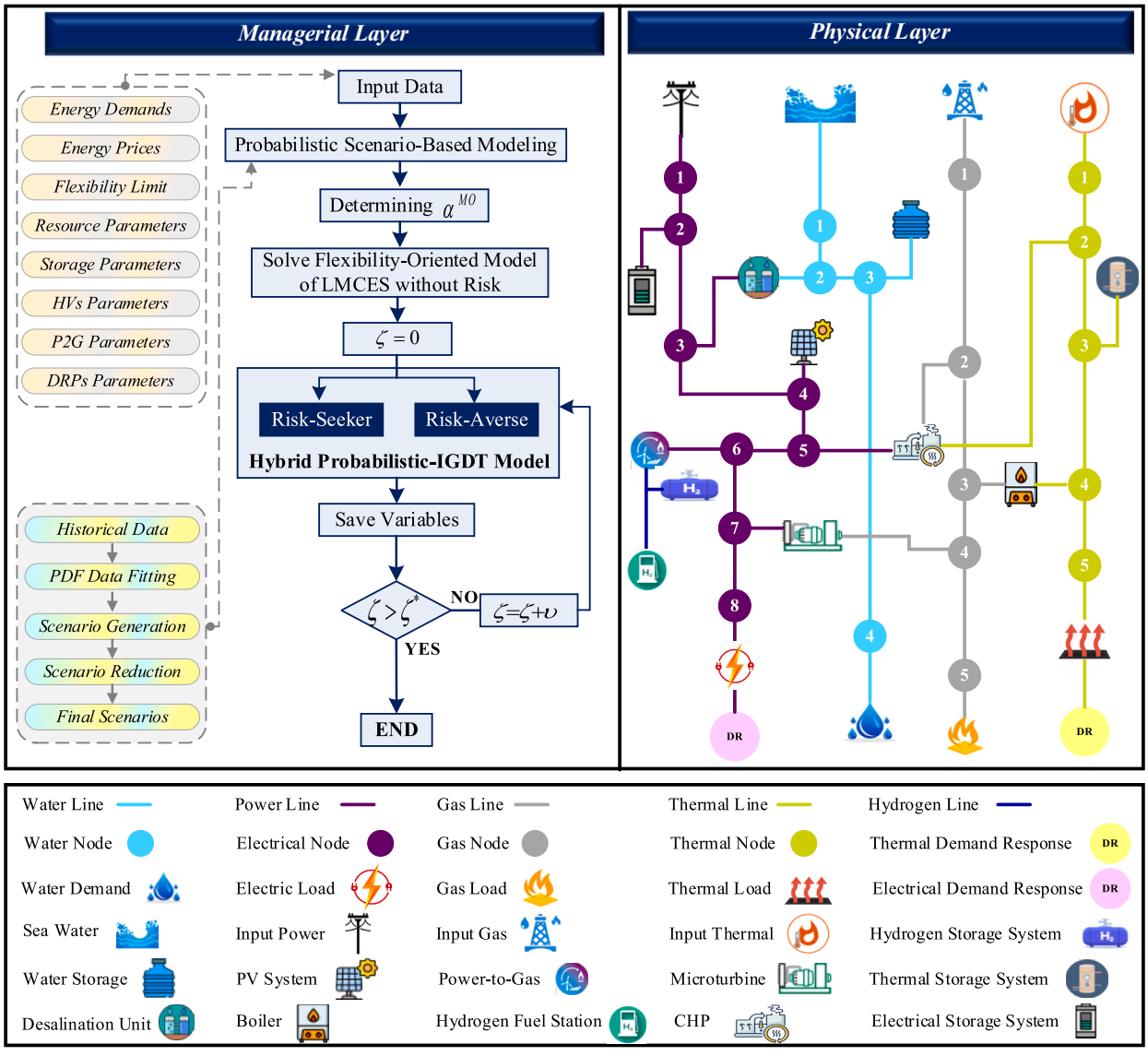


**Fig. 1.** The conceptual physical and managerial layers of the proposed LMCES.

### 1.4. Paper organization

The paper is organized as follows: Section 2 presents the proposed model, Section 3 provides mathematical relationships and problem modeling, Section 4 implements the proposed model on a test LMCES and presents results, and the conclusion and summary of the problem are provided in the final section.

## 2. The proposed conceptual model

In this section, a conceptual framework is presented to address the operational problem of an LMCES. The proposed physical and managerial layers for optimizing the LMCES are shown in Fig. 1 while considering various objective functions.

In the managerial layer, the operator initiates the optimization process by receiving necessary data. Uncertainties related to the PV system, electricity prices, and electrical and heat loads are then modeled using a scenario-based approach. In this regards, historical data is collected for uncertain parameters and modeled using a Probability Density Function (PDF). The Monte Carlo method is used to generate the required number of scenarios, which are then reduced using the K-means method. The reduced scenarios and other necessary data are input into the GAMS software for optimization. The multi-objective parameter, $a^{MO}$, is determined by the LMCES owner, and a flexibility-oriented probabilistic model is solved to achieve a no-risk operational cost. This calculated cost is then utilized in the probabilistic-IGDT optimization approach. Subsequently, the operation cost division factor, $\zeta$, is set to zero, and the proposed probabilistic IGDT optimization approach is solved based on the LMCES owner's risk attitude. The results are saved and then $\zeta$ is incremented by a specific amount, with the probabilistic IGDT optimization being resolved iteratively until $\zeta$ reaches $\zeta^{*}$.

In the physical layer, the LMCES imports electrical, heat, gas, and seawater resources. The inclusion of seawater and a desalination unit ensures a reliable and sustainable supply of freshwater, particularly in regions with limited access to freshwater resources but proximity to the sea. The desalination unit converts seawater into potable water, reducing dependency on external freshwater sources. To further enhance its self-sufficiency, the LMCES incorporates storage systems for electrical energy, heat energy, water, and hydrogen. Notably, due to the consistent price of gas, there is no economic advantage in storing gas, and as such, the system does not include a gas storage component. Additionally, to optimize the operational costs, the LMCES implements electrical and heat demand response programs. Furthermore, the integration of a P2G unit and a hydrogen fuel station unit allows for the conversion of excess electrical energy into hydrogen, meeting the demands of hydrogen vehicles and supporting the transition to clean transportation while reducing reliance on fossil fuels.

Furthermore, it is important to highlight that while the concepts of flexibility and reserve are commonly discussed concerning large-scale power systems, this paper intentionally excludes these indices from the proposed framework. The main rationale for this omission is the specific focus and scope of this paper, which is centered on local energy systems. The LMCES considered in this study is comparable to small communities or neighbourhood-scale systems, emphasizing tailored solutions that cater to their unique operational dynamics and constraints. However, technical scalability can be achieved by replicating and integrating model components, while operational scalability involves aggregating multiple LMCESs and implementing hierarchical controls. Moreover, the proposed incentive-based mechanism is adaptable to different scales. As the community size increases, the parameters within the flexibility constraints can be adjusted to maintain efficiency and effectiveness, ensuring the model remains robust across various scales. The framework put forth here provides a platform for LMCESs to interact with the flexibility of the upstream network, thereby improving the overall flexibility of the power system. However, it should be noted that the flexibility and reserve of the upstream network may be influenced by several factors such as energy storage systems, fast ramp resources, and DRPs, which are beyond the scope of this paper.

The successful implementation of the proposed model for LMCESs is influenced by various policy and regulatory factors. Understanding these influences is crucial for practical adoption and deployment. The integration of DERs and flexibility programs is often subject to national and regional energy policies. Policies such as renewable energy incentives, carbon pricing, and grid modernization initiatives play a significant role in shaping the operational environment for LMCESs. The proposed model aligns with several existing policies aimed at promoting renewable energy and reducing greenhouse gas emissions. However, the model's effectiveness could be influenced by regulatory frameworks that dictate the operational flexibility of LMCESs. For instance, policies that provide financial incentives for flexibility or impose penalties for non-compliance could affect the willingness of LMCES operators to engage in flexibility programs. Barriers such as stringent regulatory requirements or lack of supportive infrastructure could impede the model's implementation. Conversely, there are opportunities for policy development that could enhance model adoption. These include introducing supportive regulations for energy management systems and flexibility programs, as well as providing subsidies or tax benefits for technologies integrated within LMCESs.

## 3. Mathematical modeling

The following section outlines the mathematical model for the proposed framework. Initially, the discussion focuses on the multi-objective probabilistic optimization model. Subsequently, the epsilon constraint method is utilized to resolve the multi-objective approach, ensuring effective decision-making under uncertainty. To accommodate the risk attitudes of the LMCES owner when faced with uncertainty, the third subsection introduces the hybrid probabilistic-IGDT approach.

### 3.1. Multi-objective probabilistic optimization model

In this subsection, a detailed presentation of the probabilistic formulations of the LMCES scheduling problem is provided. The multi-objective LMCES scheduling model, as shown in Eq. (1), consists of two objective functions. The first objective function is expressed in dollars ($) as its unit of measurement, while the second objective function is expressed in kilograms (kg).

$$Minimize: \quad \left\{\psi^{\mathrm{Cost}}, \psi^{Emi}\right\} \tag{1}$$

The economic objective function, as described in Eq. (2), comprises different components outlined in Eqs. (3)–(8). The costs associated with the exchange of power, heat, and gas energies with the upstream network are represented by Eqs. (3)–(5). The flexibility cost or profit of the LMCES, based on its participation in the flexibility program, is modeled by Eq. (6). In this regard, the default ramp rate for electrical energy trading (denoted as $\zeta^{\mathrm{Def}}$) is determined by the upstream system operator, while the LMCES endeavors to calculate the optimal ramp rate for electrical energy trading (denoted as $\zeta^{\mathrm{Flex}}_{i,s,t}$) taking into account the flexibility price ($\pi^{\mathrm{Flex}}$) and other relevant parameters. The cost of participation in electrical and heat DRPs is delineated in Eqs. (7) and (8), respectively. The extent of upward and downward load shifting is contingent on the fixed price and the amount of the load factor.

$$\Psi^{Cost}: \sum_{t=1}^{N_t}\sum_{s=1}^{N_S}\omega_s\left[Cost^{E}_{t,s}+Cost^{H}_{t,s}+Cost^{G}_{t,s}+Cost^{Flex}_{t,s}+Cost^{EDR}_{t,s}+Cost^{TDR}_{t,s}\right] \tag{2}$$

where:

$$\mathrm{Cost}^{\mathrm{E}}_{t,s} = \sum_{\substack{i=1 \\ i\in ESP}}^{N_i} \pi^{\mathrm{E}}_{t,s}\left(P^{\mathrm{E,b}}_{i,t,s} - P^{\mathrm{E,S}}_{i,t,s}\right) \tag{3}$$

$$\mathrm{Cost}^{\mathrm{H}}_{t,s} = \sum_{\substack{f=1 \\ f\in HSP}}^{N_f} \pi^{\mathrm{H}}_{t,s}\left(P^{\mathrm{H,b}}_{f,t,s} - P^{\mathrm{H,S}}_{f,t,s}\right) \tag{4}$$

$$\mathrm{Cost}^{\mathrm{G}}_{t,s} = \sum_{\substack{m=1 \\ m\in GSP}}^{N_m} \pi^{\mathrm{G}}\left(P^{\mathrm{G,b}}_{m,t,s}\right) \tag{5}$$

$$\mathrm{Cost}^{\mathrm{Flex}}_{t,s} = \sum_{\substack{i=1 \\ i\in ESP}}^{N_i} \pi^{\mathrm{Flex}}\left(\zeta^{\mathrm{Flex}}_{i,s,t} - \zeta^{\mathrm{Def}}\right) \tag{6}$$

$$\mathrm{Cost}^{\mathrm{EDR}}_{t,s} = \sum_{\substack{i=1 \\ i\in ESP}}^{N_i} \left(\pi^{\mathrm{E,up}}\frac{EL_{i,t,s}}{EL^{Peak}_{i,t,s}}\mu^{\mathrm{E,up}}_{i,t,s} + \pi^{\mathrm{E,dn}}\frac{EL_{i,t,s}}{EL^{Peak}_{i,t,s}}\mu^{\mathrm{E,dn}}_{i,t,s}\right) \tag{7}$$

$$\mathrm{Cost}^{\mathrm{TDR}}_{t,s} = \sum_{\substack{f=1 \\ f\in HSP}}^{N_f} \left(\pi^{\mathrm{T,up}}\frac{TL_{f,t,s}}{TL^{\mathrm{Peak}}_{f,t,s}}\mu^{\mathrm{T,up}}_{f,t,s} + \pi^{\mathrm{T,dn}}\frac{TL_{f,t,s}}{TL^{Peak}_{f,t,s}}\mu^{\mathrm{T,dn}}_{f,t,s}\right) \tag{8}$$

The second objective function, as described in Eq. (9), pertains to the emissions generated by various resources including the CHP unit, boiler, gas load, upstream power, and microturbine. These emissions are quantified by Eqs. (10)–(14), respectively.

$$\Psi^{\mathrm{Emi}} : \sum_{t=1}^{N_t}\sum_{s=1}^{N_s} \omega_s\left(\phi^{\mathrm{CHP}}_{t,s} + \phi^{\mathrm{Boiller}}_{t,s} + \phi^{\mathrm{G}}_{t,s} + \phi^{\mathrm{Net}}_{t,s} + \phi^{\mathrm{MT}}_{t,s}\right) \tag{9}$$

where:

$$\phi^{\mathrm{CHP}}_{t,s} = \sum_{i=1}^{N_i}\left[\left(\chi^{\mathrm{CO,CHP}}P^{\mathrm{CHP}}_{i,t,s}\right) + \left(\chi^{\mathrm{SO,CHP}}P^{\mathrm{CHP}}_{i,t,s}\right) + \left(\chi^{\mathrm{NO,CHP}}P^{\mathrm{CHP}}_{i,t,s}\right)\right] \tag{10}$$

$$\phi^{\mathrm{Boiller}}_{t,s} = \sum_{f=1}^{N_f}\left[\left(\chi^{\mathrm{CO,Boiller}}H^{\mathrm{B}}_{f,t,s}\right) + \left(\chi^{\mathrm{SO,Boiller}}H^{\mathrm{B}}_{f,t,s}\right) + \left(\chi^{\mathrm{NO,Boiller}}H^{\mathrm{B}}_{f,t,s}\right)\right] \tag{11}$$

$$\phi^{\mathrm{G}}_{t,s} = \sum_{m=1}^{N_m}\left[\left(\chi^{\mathrm{CO,G}}GL_{m,t,s}\right) + \left(\chi^{\mathrm{SO,G}}GL_{m,t,s}\right) + \left(\chi^{\mathrm{NO,G}}GL_{m,t,s}\right)\right] \tag{12}$$

$$\phi^{\mathrm{NET}}_{t,s} = \sum_{i=1}^{N_i}\left[\left(\chi^{\mathrm{CO,NET}}P^{\mathrm{E,b}}_{i,t,s}\right) + \left(\chi^{\mathrm{SO,NET}}P^{\mathrm{E,b}}_{i,t,s}\right) + \left(\chi^{\mathrm{NO,NET}}P^{\mathrm{E,b}}_{i,t,s}\right)\right] \tag{13}$$

$$\phi^{\mathrm{MT}}_{t,s} = \sum_{i=1}^{N_i}\left[\left(\chi^{\mathrm{CO,MT}}P^{\mathrm{MT}}_{i,t,s}\right) + \left(\chi^{\mathrm{SO,MT}}P^{\mathrm{MT}}_{i,t,s}\right) + \left(\chi^{\mathrm{NO,MT}}P^{\mathrm{MT}}_{i,t,s}\right)\right] \tag{14}$$

The LMCES features a CHP unit that is capable of concurrently generating electricity and heat. The operational setup of the CHP unit is defined by a set of inequalities (15)–(20). These inequalities model the feasible generating region of the CHP unit, ensuring that both power and heat output energies fall within specified limits (18) and (19) respectively, while also considering the gas consumption of the CHP unit by (20).

$$P^{\mathrm{CHP}}_{i,t,s} - P^{\mathrm{A,CHP}} - \frac{P^{\mathrm{A,CHP}} - P^{\mathrm{B,CHP}}}{H^{\mathrm{A,CHP}} - H^{\mathrm{B,CHP}}}\left(H^{\mathrm{CHP}}_{f,t,s} - H^{\mathrm{A,CHP}}\right) \le 0 \tag{15}$$

$$P^{\mathrm{CHP}}_{i,t,s} - P^{\mathrm{B,CHP}} - \frac{P^{\mathrm{B,CHP}} - P^{\mathrm{C,CHP}}}{H^{\mathrm{B,CHP}} - H^{\mathrm{C,CHP}}}\left(H^{\mathrm{CHP}}_{f,t,s} - H^{\mathrm{B,CHP}}\right) \ge -\left(1 - I^{\mathrm{CHP}}_{i,t,s}\right)\times M \tag{16}$$

$$P^{\mathrm{CHP}}_{i,t,s} - P^{\mathrm{C,CHP}} - \frac{P^{\mathrm{C,CHP}} - P^{\mathrm{D,CHP}}}{H^{\mathrm{C,CHP}} - H^{\mathrm{D,CHP}}}\left(H^{\mathrm{CHP}}_{f,t,s} - H^{\mathrm{C,CHP}}\right) \ge -\left(1 - I^{\mathrm{CHP}}_{i,t,s}\right)\times M \tag{17}$$

$$0 \le H^{\mathrm{CHP}}_{f,t,s} \le H^{\mathrm{B,CHP}}I^{\mathrm{CHP}}_{i,t,s} \tag{18}$$

$$0 \le P^{\mathrm{CHP}}_{i,t,s} \le P^{\mathrm{A,CHP}}I^{\mathrm{CHP}}_{i,t,s} \tag{19}$$

$$P^{\mathrm{CHP}}_{i,t,s} = GC^{\mathrm{CHP}}_{m,t,s}\delta^{\mathrm{CHP}} \tag{20}$$

The quantity of gas utilized by the microturbine unit, as well as the power generated, are stated by Eqs. (21) and (22) respectively [46].

$$P^{\mathrm{MT}}_{i,t,s} = GC^{\mathrm{MT}}_{m,t,s}\delta^{\mathrm{MT}} \tag{21}$$

$$0 \le P^{\mathrm{MT}}_{i,t,s} \le \overline{P}^{\mathrm{MT}} \tag{22}$$

The management of performance constraints for the boiler unit is addressed through the utilization of Eq. (23) and inequality (24) [47].

$$H^{\mathrm{B}}_{f,t,s} = GB^{\mathrm{B}}_{m,t,s}\delta^{\mathrm{B}} \tag{23}$$

$$\underline{H}^{\mathrm{B}}I^{\mathrm{B}}_{t,s} \le H^{\mathrm{B}}_{f,t,s} \le \overline{H}^{\mathrm{B}}I^{\mathrm{B}}_{f,t,s} \tag{24}$$

Charging and discharging power constraints of the electric energy storage are modeled by (25)–(28), while constraints (29)–(32) stand for the heat energy storage unit [48].

$$SOC^{\mathrm{ES}}_{i,t,s} = SOC^{\mathrm{ES}}_{i,t-1,s} + \eta^{\mathrm{ES}}PE^{\mathrm{ch,ES}}_{i,t,s} - PE^{\mathrm{dis,ES}}_{i,t,s}\left(1/\eta^{\mathrm{ES}}\right) \tag{25}$$

$$\underline{SOC}^{\mathrm{ES}} \le SOC^{\mathrm{ES}}_{i,t,s} \le \overline{SOC}^{\mathrm{ES}} \tag{26}$$

$$0 \le PE^{\mathrm{ch,ES}}_{i,t,s} \le I^{\mathrm{ES}}_{i,t,s}\overline{PE}^{\mathrm{ch,ES}} \tag{27}$$

$$0 \le PE^{\mathrm{dis,ES}}_{i,t,s} \le \left(1 - I^{\mathrm{ES}}_{i,t,s}\right)\overline{PE}^{\mathrm{dis,ES}} \tag{28}$$

$$SOC^{\mathrm{TS}}_{f,t,s} = SOC^{\mathrm{TS}}_{f,t-1,s} + \eta^{\mathrm{TS}}PH^{\mathrm{ch,TS}}_{f,t,s} - PH^{\mathrm{dis,TS}}_{f,t,s}\left(1/\eta^{\mathrm{TS}}\right) \tag{29}$$

$$\underline{SOC}^{\mathrm{TS}} \le SOC^{\mathrm{TS}}_{f,t,s} \le \overline{SOC}^{\mathrm{TS}} \tag{30}$$

$$0 \le PH^{\mathrm{ch,TS}}_{f,t,s} \le I^{\mathrm{TS}}_{f,t,s}\overline{PH}^{\mathrm{ch,TS}} \tag{31}$$

$$0 \le PH^{\mathrm{dis,TS}}_{f,t,s} \le \left(1 - I^{\mathrm{TS}}_{f,t,s}\right)\overline{PH}^{\mathrm{dis,TS}} \tag{32}$$

The transfer of diverse energy transactions with the upstream network, including electricity, heat, and gas, is restricted by Eqs. (33)–(37). The quantity of electric / heat energy sold to and purchased from the upstream network is regulated by Eqs. (33) and (34) / Eqs. (35) and (36); the level of required gas from the upstream gas network is limited by (37).

$$0 \le P^{\mathrm{E,b}}_{i,t,s} \le \overline{P}^{\mathrm{E,b}}I^{\mathrm{E}}_{i,t,s} \tag{33}$$

$$0 \le P^{\mathrm{E,S}}_{i,t,s} \le \overline{P}^{\mathrm{E,S}}\left(1 - I^{\mathrm{E}}_{i,t,s}\right) \tag{34}$$

$$0 \le P^{\mathrm{H,b}}_{f,t,s} \le \overline{P}^{\mathrm{H,b}}I^{\mathrm{H}}_{f,t,s} \tag{35}$$

$$0 \le P^{\mathrm{H,S}}_{f,t,s} \le \overline{P}^{\mathrm{H,S}}\left(1 - I^{\mathrm{H}}_{f,t,s}\right) \tag{36}$$

$$0 \le P^{G}_{m,t,s} \le \overline{P}^{G} \tag{37}$$

The challenges posed by the constraints of gas flow within pipelines are inherently characterized by strong nonlinearity, leading to non-convexity within the feasible region. In addressing this issue, this paper specifically focuses on the examination of gas flow limitations in gas pipelines as outlined in Eq. (38), with the aim of mitigating potential non-convexity [49].

$$\underline{F}^{G} \le F^{G}_{m,n,t,s} \le \overline{F}^{G} \tag{38}$$

The LMCEC is characterized by a relatively small and localized configuration. Consequently, gas pressure fluctuations within the LMCES are considered negligible and therefore are excluded from calculations [49]. However, limitations of electrical, heat, and water flow are addressed through Eqs. (39)–(41) as referenced in [3,50].

$$\underline{F}^{EL} \le F^{EL}_{i,j,t,s} \le \overline{F}^{EL} \tag{39}$$

$$\underline{F}^{H} \le F^{H}_{f,g,t,s} \le \overline{F}^{H} \tag{40}$$

$$\underline{F}^{W} \le F^{W}_{p,q,t,s} \le \overline{F}^{W} \tag{41}$$

The fluctuations in energy exchange between the LMCES and the upstream network have been found to significantly disrupt the flexibility of the upstream network. To address this issue, a prescribed flexibility constraint has been introduced to mitigate the excessive variability in energy exchange rates. This constraint aims to ensure a more consistent and controlled flow of energy between the LMCES and the upstream network, thereby enhancing the overall smoothness and efficiency of the energy exchange process. The proposed flexibility constraint, denoted as Eq. (42), is inherently nonlinear; however, it can be transformed into a linear form through the application of auxiliary constraints as represented by Eqs. (43) and (44).

$$\left|\left(P^{E,b}_{i,s,t} - P^{E,b}_{i,t-1,s}\right) - \left(P^{E,S}_{i,s,t} - P^{E,S}_{i,t-1,s}\right)\right| \le \zeta^{Flex}_{i,s,t} \tag{42}$$

$$\left(P^{E,b}_{i,s,t} - P^{E,b}_{i,t-1,s}\right) - \left(P^{E,S}_{i,s,t} - P^{E,S}_{i,t-1,s}\right) \le \zeta^{Flex}_{i,s,t} \tag{43}$$

$$-\left(P^{E,b}_{i,s,t} - P^{E,b}_{i,t-1,s}\right) + \left(P^{E,S}_{i,s,t} - P^{E,S}_{i,t-1,s}\right) \le \zeta^{Flex}_{i,s,t} \tag{44}$$

The utilization of Hydrogen Vehicles (HVs) has been acknowledged as an effective approach to reduce greenhouse gas emissions and enhance the overall operational efficiency of transportation systems. Nevertheless, the infrastructure for providing hydrogen fuel to support these vehicles is currently underdeveloped. To address this pressing issue, the proposal involves the establishment of an on-site hydrogen fueling station. This facility operates independently from the existing gas network and relies on a P2G unit in combination with a hydrogen storage tank to meet the required hydrogen demand. The equilibrium of hydrogen within this system is mathematically modeled using Eq. (45), taking into account various parameters such as hydrogen production, storage injection and absorption, and consumption by the fleet of vehicles. Recognizing that arriving vehicles may possess diverse states of charge, a stochastic parameter is incorporated into Eq. (46) to accurately capture the demand of each vehicle. Additionally, the output of P2G unit, which depends on the efficiency of the electrolysis process and operating temperature, is determined by Eq. (47).

$$HG^{P2G}_{s,t} + HG^{dis,HTS}_{s,t} - HG^{ch,HTS}_{s,t} = \sum_{v=1}^{N_v} HG^{HV}_{s,v,t} \tag{45}$$

$$HG^{HV}_{s,v,t} = Rand(0,1) \times VT \tag{46}$$

$$HG^{P2G}_{s,t} \le \frac{P^{P2G}_{i,s,t}\eta^{P2G}}{HHV} \tag{47}$$

The hydrogen storage system plays a crucial role in optimizing the overall energy management within LMCES. It effectively stores surplus energy from renewable resources, allowing for its utilization during periods of high demand or low renewable energy generation. Consequently, the hydrogen storage system acts as a dependable and efficient energy reservoir, ultimately enhancing the stability and resilience of the LMCES. The mathematical representation of the hydrogen storage system can be found in Eqs. (48)–(51).

$$SOC^{HTS}_{t,s} = SOC^{HTS}_{t-1,s} - HG^{dis,HTS}_{s,t} + HG^{ch,HTS}_{s,t} \tag{48}$$

$$\underline{SOC}^{HTS} \le SOC^{HTS}_{t,s} \le \overline{SOC}^{HTS} \tag{49}$$

$$0 \le HG^{ch,HTS}_{s,t} \le I^{HTS}_{t,s}\overline{PH}^{ch,HTS} \tag{50}$$

$$0 \le HG^{dis,HTS}_{s,t} \le \left(1 - I^{HTS}_{t,s}\right)\overline{PH}^{dis,HTS} \tag{51}$$

The water desalination unit is subject to specific constraints as outlined in Eqs. (52)–(54). Eq. (52) defines the parameter, denoted as $W^{W,Des}_{t,s}$, which represents the output freshwater from the desalination unit as a fraction or proportion of the input seawater; the power consumption of the desalination unit is quantified by Eq. (53); and the output water of the desalination unit is restricted by Eq. (54).

$$W^{W,Des}_{p,t,s} = W^{SW}_{p,t,s}\varpi^{EF,W} \tag{52}$$

$$W^{W,Des}_{p,t,s} = P^{Des}_{i,t,s}\eta^{EF,W} \tag{53}$$

$$0 \le W^{W,Des}_{p,t,s} \le \overline{W}^{W,Des} \tag{54}$$

The representation of the water storage system is modeled by Eqs. (55)–(58). The water level within the storage system is described by Eq. (55), which is constrained by the storage capacity outlined in Eq. (56); and the inflow and outflow of water in the storage system are controlled by Eqs. (57) and (58), respectively.

$$SOC^{WS}_{p,t,s} = SOC^{WS}_{p,t-1,s} + W^{ch,WS}_{p,t,s} - W^{dch,WS}_{p,t,s} \tag{55}$$

$$0 \le SOC^{WS}_{p,t,s} \le \overline{SOC}^{WS} \tag{56}$$

$$0 \le W^{ch,WS}_{p,t,s} \le I^{WS}_{p,t,s}\overline{W}^{ch,WS} \tag{57}$$

$$0 \le W^{dch,WS}_{p,t,s} \le \left(1 - I^{WS}_{p,t,s}\right)\overline{W}^{dch,WS} \tag{58}$$

The equilibrium of electrical, heat, gas, and water loads is addressed by Eqs. (59)–(62), respectively.

$$P^{E,b}_{i,t,s} - P^{E,S}_{i,t,s} + P^{MT}_{i,t,s} + P^{CHP}_{i,t,s} - PE^{Ch,E,S}_{i,t,s} + PE^{dis,E,S}_{i,t,s} + P^{PV}_{i,t,s} - P^{P2G}_{i,t,s} - P^{Des}_{i,t,s} + \sum_{j=1}^{N_j} F^{EL}_{i,j,t,s} = EL^{DR}_{i,t,s} \tag{59}$$

$$P^{H,b}_{f,t,s} - P^{H,S}_{f,t,s} - PH^{ch,TS}_{f,t,s} + PH^{dis,TS}_{f,t,s} + H^{CHP}_{f,t,s} + H^{B}_{f,t,s} + \sum_{g=1}^{N_g} F^{H}_{f,g,t,s} = TL^{DR}_{f,t,s} \tag{60}$$

$$P^{G}_{m,t,s} - GB^{B}_{m,t,s} - GC^{CHP}_{m,t,s} - GC^{MT}_{m,t,s} + \sum_{n=1}^{N_n} F^{G}_{m,n,t,s} = GL_{m,t,s} \tag{61}$$

$$W^{W,Des}_{p,t,s} + W^{dch,WS}_{p,t,s} - W^{ch,WS}_{p,t,s} + \sum_{q=1}^{N_q} P^{W}_{p,q,t,s} = WL_{p,t,s} \tag{62}$$

### 3.2. Multi-objective solving approach

The mathematical model proposed for LMCES presents a complex multi-objective optimization problem, which calls for the application of an MCDM approach for resolution. Among the various methods available for addressing multi-objective optimization problems, the epsilon constraint method stands out as a popular choice. This method involves designating one objective as the primary focus for optimization, typically the most critical one, while the remaining objectives are transformed into constraints. By optimizing the primary objective within the constraints set by the other objectives, a balance can be achieved in addressing conflicting goals. In the context of this study, the operational cost has been identified as the primary objective to be prioritized in the multi-objective function. As a result, the proposed multi-objective function has been redefined to reflect this prioritization as follows.

$$Min\Psi^{Cost}: \sum_{t=1}^{N_t}\sum_{s=1}^{N_S}\omega_s\left[Cost_{t,s}^{E}+Cost_{t,s}^{H}+Cost_{t,s}^{G}+Cost_{t,s}^{Flex}+Cost_{t,s}^{EDR}+Cost_{t,s}^{TDR}\right] \tag{63}$$

s.t

$$\Psi^{Emi}: \sum_{t=1}^{N_t}\sum_{s=1}^{N_s}\omega_s\left(\phi_{t,s}^{CHP}+\phi_{t,s}^{Boiller}+\phi_{t,s}^{G}+\phi_{t,s}^{Net}+\phi_{t,s}^{MT}\right)\le\left(1-a^{MO}\right)\varepsilon \tag{64}$$

$$\text{bad hbox}^{Cost}: \sum_{t=1}^{N_t}\sum_{s=1}^{N_s}\omega_s\left[\text{Cost}_{t,s}^{E}+\text{Cost}_{t,s}^{H}+\text{Cost}_{t,s}^{G}+\text{Cost}_{t,s}^{Flex}+\text{Cost}_{t,s}^{EDR}+\text{Cost}_{t,s}^{TDR}\right] \leqslant \text{Cost}^{\text{bad hbox}}(1+\zeta) \tag{69}$$

Constraints (3-8), (10-62) and (A1)-(A10). (65)

Incorporating a parameter known as epsilon ($\varepsilon$) into the approach is an essential element, as it represents the maximum allowable deviation from the optimal solution for each constraint. Moreover, $a^{MO}$ signifies the acceptable tolerance level for the second objective function.

### 3.3. Hybrid probabilistic-IGDT model

The proposed hybrid probabilistic-IGDT model has been developed to effectively capture the uncertainty in both renewable energy resources and decision-making processes. This model not only considers the stochastic nature of PV generation as a clean energy system but also integrates the uncertainty associated with the risk attitudes of LMCES operators. Combining probabilistic techniques with IGDT, it offers a more comprehensive understanding of the factors influencing operational costs and emission production, thereby ensuring practical applicability and robustness of the solutions.

In dealing with the uncertainty set of the PV system, the model adopts an envelope-bound uncertainty approach, enabling a thorough exploration of the potential range of outcomes.

$$U\left(\widetilde{P}_{i,t,s}^{PV},a^{PV}\right)=\left\{P_{i,t,s}^{PV}:\left|P_{i,t,s}^{PV}-\widetilde{P}_{i,t,s}^{PV}\right|\le a^{PV}\widetilde{P}_{i,t,s}^{PV}\right\} \tag{66}$$

where, $a^{PV}$ is the uncertainty horizon variable, $\widetilde{P}_{i,t,s}^{PV}$ and $P_{i,t,s}^{PV}$ are the forecasted power parameter and the output uncertainty variable of the PV system, respectively. The linear type of Eq. (66) can be expressed as follows:

$$\widetilde{P}_{i,t,s}^{PV}\left(1-a^{PV}\right)\le P_{i,t,s}^{PV}\le\left(1+a^{PV}\right)\widetilde{P}_{i,t,s}^{PV} \tag{67}$$

When faced with the uncertainty of PV, the LMCES operator may demonstrate either risk-averse or risk-seeking behavior. The subsequent sections will delve into the mathematical expressions for both risk-averse and risk-seeking approaches.

#### 3.3.1. Risk-averse strategy

In the risk-averse strategy, the focus lies on maximizing the uncertain variable $a^{PV}$. Furthermore, it is crucial to ensure that the maximum potential cost associated with LMCES remains below the no-risk expenditure ($\text{Cost}^{\text{No\_Risk}}$). To achieve the maximum cost of the LMCES, careful consideration of risk factors, $\left(1-a^{PV}\right)\widetilde{P}_{i,t,s}^{PV}$, is essential in the optimization problem. Consequently, the optimization problem can be restated as follows:

$$Max\ a^{PV} \tag{68}$$

s.t

$$P_{i,t,s}^{E,b}-P_{i,t,s}^{E,S}+P_{i,t,s}^{MT}+P_{i,t,s}^{CHP}-PE_{i,t,s}^{Ch,E,S}+PE_{i,t,s}^{dis,E,S}+\left(1-a^{pv}\right)\widetilde{P}_{i,t,s}^{PV}-P_{i,t,s}^{P2G}-P_{i,t,s}^{Des}+\sum_{j=1}^{N_j}F_{i,j,t,s}^{EL}=EL_{i,t,s}^{DR} \tag{70}$$

(71) Constraints (3)–(8), (10)–(68), (70)–(72) and (74).

#### 3.3.2. Risk-seeker strategy

The risk-seeking LMCES operator adopts an approach to uncertain events with the goal of optimizing outcomes positively. In this strategy, the LMCES operator involves an optimistic outlook, and his aim is to minimize the $a^{PV}$, ensuring that the LMCES cost is lower than the no-risk cost ($\text{Cost}^{\text{No\_Risk}}$). In order to achieve the minimum LMCES cost, $\left(1+a^{PV}\right)\widetilde{P}_{i,t,s}^{PV}$is considered in the optimization problem.

$$Min\ a^{PV} \tag{72}$$

s.t

$$\text{bad hbox}^{Cost}: \sum_{t=1}^{N_t}\sum_{s=1}^{N_s}\omega_s\left[\text{Cost}_{t,s}^{E}+\text{Cost}_{t,s}^{H}+\text{Cost}_{t,s}^{G}+\text{Cost}_{t,s}^{Flex}+\text{Cost}_{t,s}^{EDR}+\text{Cost}_{t,s}^{TDR}\right] \leqslant \text{Cost}^{\text{bad hbox}}(1-\zeta) \tag{73}$$

s.t

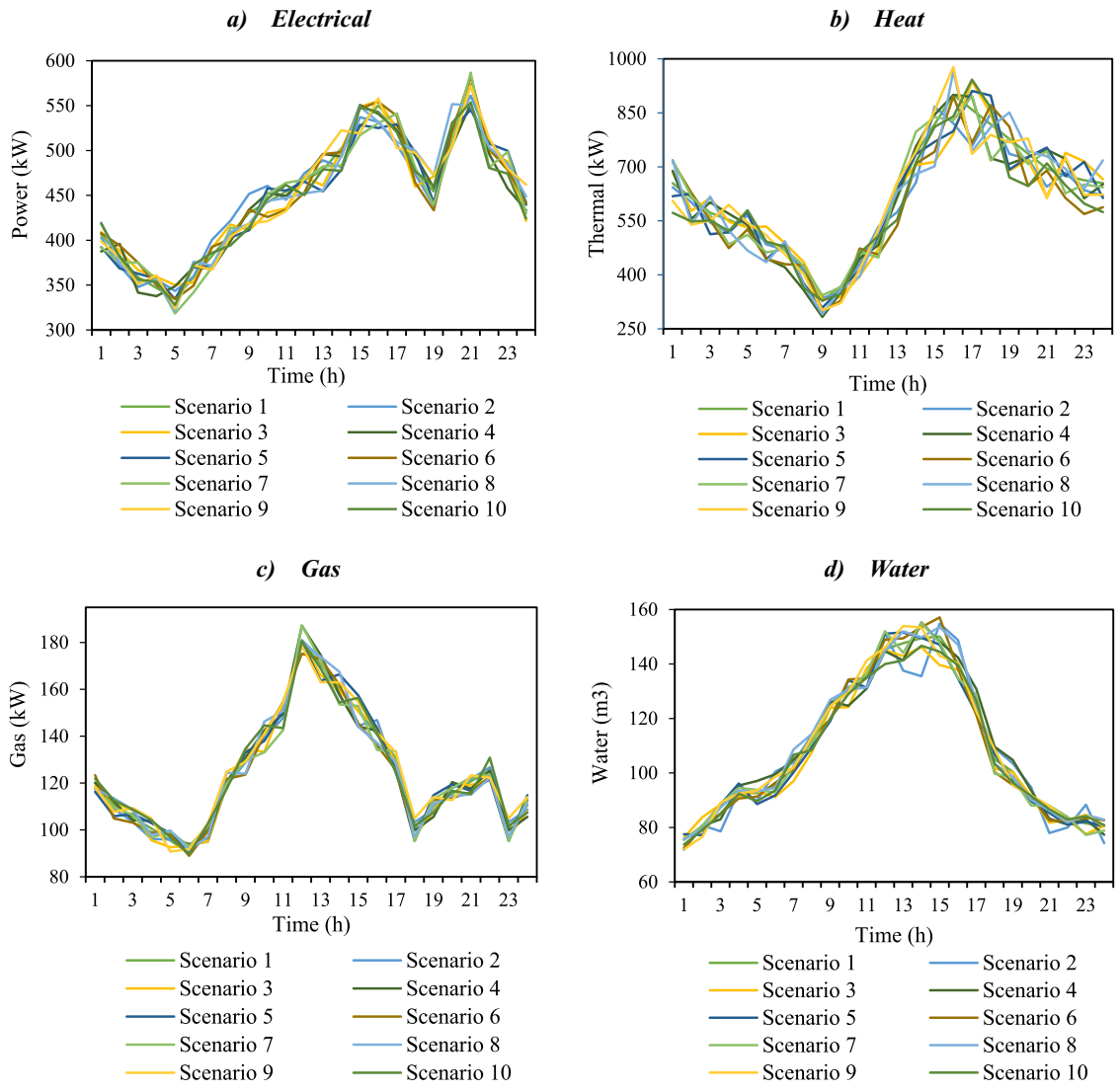


**Fig. 2.** The energy demands: a) Electrical demand, b) Heat demand, c) Gas demand and d) Water demand.

$$P^{E,b}_{i,t,s} - P^{E,S}_{i,t,s} + P^{MT}_{i,t,s} + P^{CHP}_{i,t,s} - PE^{Ch,E,S}_{i,t,s} + PE^{dis,E,S}_{i,t,s} + (1-\alpha^{pv})\widetilde{P}^{PV}_{i,t,s} - P^{P2G}_{i,t,s} - P^{Des}_{i,t,s} + \sum_{j=1}^{N_j} F^{EL}_{i,j,t,s} = EL^{DR}_{i,t,s} \quad (74)$$

Constraints (3)–(8), (10)–(58), (60)–(62) and (64) and (A1)–(A10) (75)

**Table 3**
The electrical, heat, and water energy storage parameters.

| Parameter | Value | Parameter | Value |
|---|---|---|---|
| $\underline{SOC}^{ES}$ | 0 | $\underline{SOC}^{TS}$ | 0 |
| $\overline{SOC}^{ES}$ | 300 | $\overline{SOC}^{TS}$ | 300 |
| $\overline{PE}^{ch,ES}$ | 100 | $\overline{PE}^{ch,TS}$ | 100 |
| $\overline{PE}^{dis,ES}$ | 100 | $\overline{PE}^{dis,TS}$ | 100 |
| $\eta^{ES}$ | 0.98 | $\eta^{TS}$ | 0.98 |
| $SOC^{WS}_{max}$ | 200 | $W^{ch,WS}_{max}$ | 50 |
| $W^{dch,WS}_{max}$ | 50 | $\pi^{G}$ | 0.072 |

## 4. Numerical study

This section focuses on implementing the proposed optimization model on a sample LMCES as depicted in Fig. 1. The initial subsection provides a detailed explanation of the input data employed in the analysis, whereas the subsequent subsection presents the outcomes and findings of the optimization process.

### 4.1. Input data

The proposed optimization problem is a day-ahead scheduling, with hourly time intervals. The problem is formulated as a Mixed-Integer Linear Programming (MILP) optimization model and is solved using the CPLEX solver within the GAMS optimization environment. The computational process is conducted on a computer with an Intel Core i7 CPU and 16 GB of RAM.

The electrical, heat, gas, and water requirements of the LMCES are depicted in Fig. 2. It is observed that the system experiences its highest demand for electricity at hour 21. Consequently, the LMCES operator is compelled to explore effective strategies to manage this surge in demand. Additionally, it is noteworthy that the peak load for heat occurs between hours 15 and 19, with periods of low demand observed between hours 8 and 10. Moreover, it is significant to acknowledge that the peak periods for gas and water consumption predominantly occur

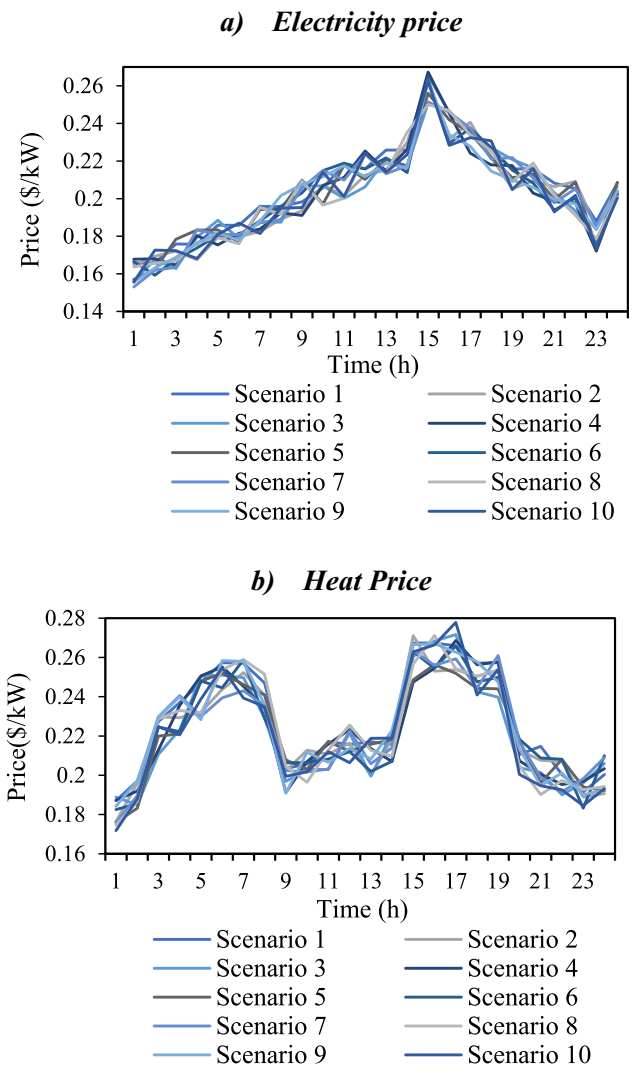


**Fig. 3.** The energy prices: a) electricity price and b) Heat price.

**Table 4**
The input fixed parameters of the CHP, microturbine, and boiler units [52].

| Parameter | Value | Parameter | Value |
|---|---|---|---|
| $P_{A}^{CHP}$ | 263 (kW) | $H_{C}^{CHP}$ | 120 (kW) |
| $P_{B}^{CHP}$ | 195 (kW) | $H_{D}^{CHP}$ | 0 (kW) |
| $P_{C}^{CHP}$ | 45 (kW) | $\delta^{MT}$ | 0.35 (kW) |
| $P_{D}^{CHP}$ | 56 (kW) | $\overline{P}^{MT}$ | 100 (kW) |
| $\delta^{CHP}$ | 0.3 | $\delta^{B}$ | 0.35 |
| $H_{A}^{CHP}$ | 0 (kW) | $\underline{H}^{B}$ | 0 (kW) |
| $H_{B}^{CHP}$ | 210 (kW) | $\overline{H}^{B}$ | 50 (kW) |

**Table 5**
The emission coefficients [52].

| Parameter | Value (kg/kW) | Parameter | Value (kg/kW) | Parameter | Value (kg/kW) |
|---|---|---|---|---|---|
| $\chi^{CO,Boiler}$ | 0.37 | $\chi^{NO,Boiler}$ | 0.00009 | $\chi^{SO,Boiler}$ | 0.000003 |
| $\chi^{CO,CHP}$ | 0.37 | $\chi^{NO,CHP}$ | 0.00009 | $\chi^{SO,CHP}$ | 0.000003 |
| $\chi^{CO,G}$ | 0.37 | $\chi^{NO,G}$ | 0.00009 | $\chi^{SO,G}$ | 0.000003 |
| $\chi^{CO,Net}$ | 0.368 | $\chi^{NO,Net}$ | 0.0008 | $\chi^{SO,Net}$ | 0.0002 |
| $\chi^{CO,MT}$ | 0.37 | $\chi^{NO,MT}$ | 0.00009 | $\chi^{SO,MT}$ | 0.000003 |

**Table 6**
The P2G unit, hydrogen storage, hydrogen vehicle, and water desalination unit parameters.

| Parameter | Value | Parameter | Value |
|---|---|---|---|
| $VT$ | 0.122 | $HHV$ | 33.33 |
| $\eta^{P2G}$ | 0.6 | $\overline{SOC}^{HTS}$ | 1 |
| $\overline{PH}^{Ch,HTS}$ | 0.4 | $\underline{SOC}^{HTS}$ | 0 |
| $\overline{PH}^{Dis,HTS}$ | 0.4 | $\varpi^{EF,W}$ | 0.8 |
| $\eta^{EF,W}$ | 0.33 | $\overline{W}^{W,Des}$ | 300 |

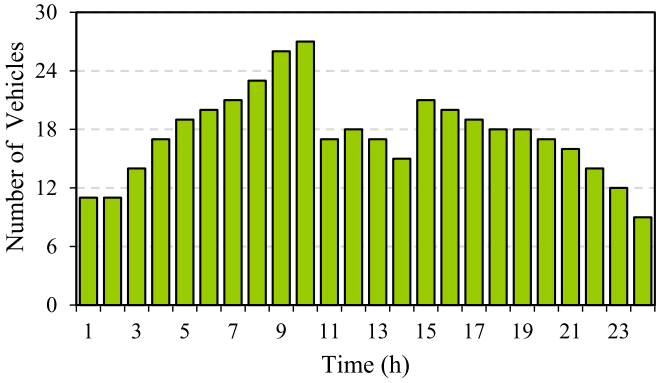


**Fig. 4.** The number of available HVs in the hydrogen fuel station.

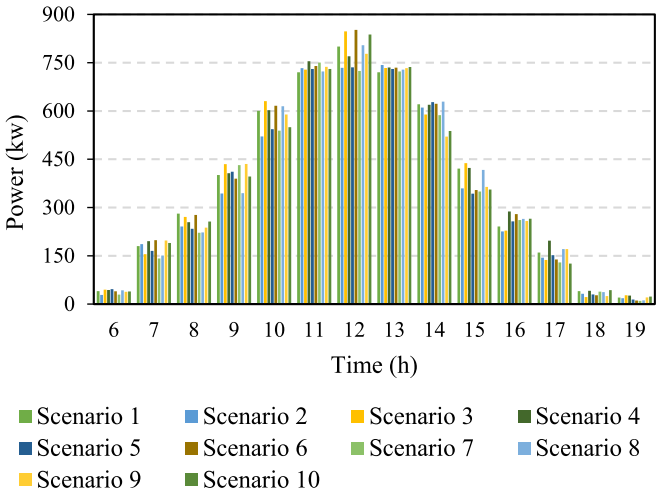


**Fig. 5.** The output power of the PV unit.

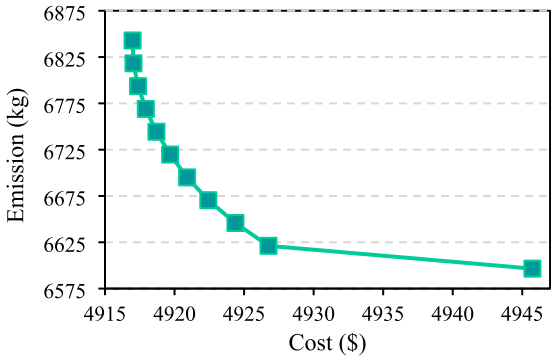


**Fig. 6.** The Pareto optimal result of operation cost and emission with increasing $a^{MO}$from 0 to $a_{*}^{MO}$.

during the midday hours.

The upper limits for both electrical and heat energy exchange with the upstream grid are set at 1000 kW each. Furthermore, the maximum gas intake from the upstream network is restricted to 1000 kW. The highest allowable levels for electrical, heat, gas and water flow in LMCES lines are 600 kW, 900 kW, 1000 kW, and 300 $m^3$, respectively. The default rate for flexibility is considered 150 kW/h. The incentive offered for participating in upward and downward DRPs in the both electrical and heat sectors is fixed at a rate of $0.02 per kilowatt (kW) [51]. The rate of participation in DRPs for electrical and heat demands is reported to be 10 % [51]. The constant parameters of electrical, heat and water energy storage are provided in Table 3.

The variability of electrical and heat energy prices in the upstream sector is a critical consideration due to their uncertain nature. As shown in Fig. 3, the output scenarios for these energy prices exhibit distinct patterns. Notably, the peak electrical energy prices are most pronounced during the time between hours 14 and 16. Similarly, the highest heat energy prices are observed within the time intervals of hours 4 to 8 and 15 to 19.

The fixed input parameter of the CHP unit can be found in Table 4, and the emission coefficients are detailed in Table 5. Additionally, Table 6 provides an overview of the input parameters for the P2G unit, hydrogen storage, and HVs. Furthermore, a visual representation of the random discrete parameter, which signifies the quantity of HVs accessible at the hydrogen fuel station, is illustrated in Fig. 4. Lastly, the output power of the PV generation unit is shown in Fig. 5.

### 4.2. Optimization results and discussions

#### 4.2.1. Probabilistic results

The following section provides an analysis of the probabilistic results obtained from the study. Referring to the epsilon constraint method, the economic target is considered the primary focus for optimization, and the environmental target is transformed into constraint. Applying the maximum acceptable deviation from the optimal solution, $\varepsilon$, and acceptable tolerance level, $a^{MO}$, the Pareto-optimal solution be achieved as illustrated in Fig. 6. It should be mentioned that $\varepsilon$ is set at 6842.88 in the optimization process and a balance between costs and emissions within the LMCES can be achieved by altering $a^{MO}$from zero to $a^{MO}_{*}$. Referring to Fig. 6, it can be observed that the economic and environmental objectives are conflicting with each other. Consequently, the operator of the LMCES is faced with the challenge of selecting an operational point that lies between the Pareto-optimal solutions. This selection necessitates a delicate balance between minimizing operational costs and reducing emissions, as the pursuit of one objective may lead to a trade-off with the other.

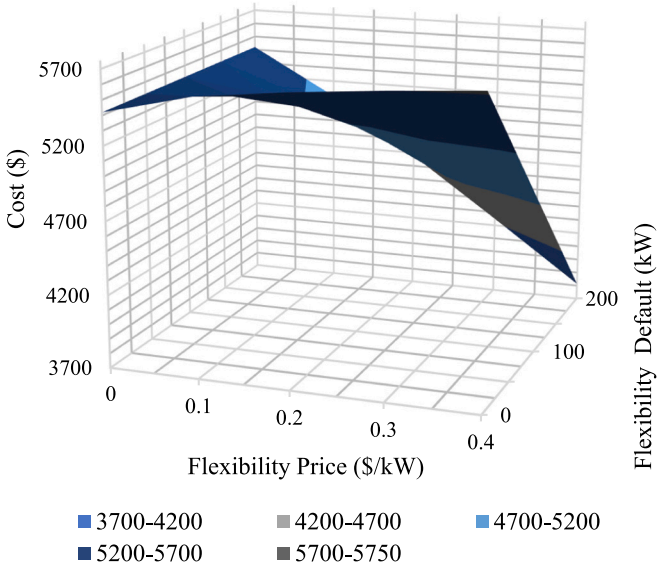


**Fig. 7.** The optimal operation cost of the LMCES with various flexibility parameters.

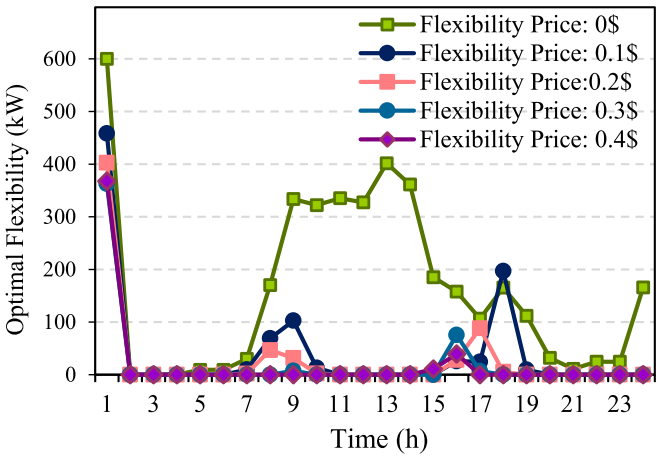


**Fig. 8.** The optimal hourly flexibility for the LMCES.

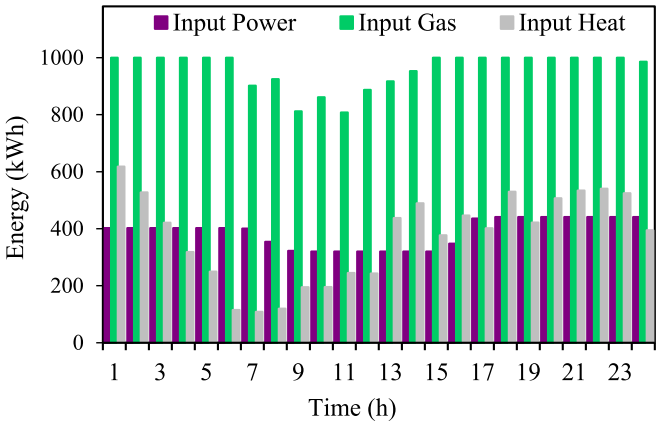


**Fig. 9.** The electrical, heat and gas energy exchange with the upstream grid.

To address the trade-off between economic and environmental objectives, the proposed LMCES model employs the Technique for Order Preference by Similarity to Ideal Solution (TOPSIS) approach as a MCDM strategy. TOPSIS is a widely recognized method for ranking and selecting from among alternatives based on their distance from an ideal solution. This approach allows for the effective balancing of economic and environmental objectives by identifying the best trade-offs between these conflicting objectives. A detailed description of the TOPSIS method can be found in [53]. Using the TOPSIS approach, the optimal operation point results in a cost of $4916.98 and emissions of 6842.88 kg.

In subsequent analysis, the outcomes are derived with consideration of the economic aspect as the highest priority, and the search space index, i.e. $a^{MO} = 0$, is set at zero.

The fundamental objective of this paper is to achieve the most efficient operation of the LMCES, considering the limitations of upstream flexibility. In this regard, the crucial factors determining the optimal operational cost of the LMCES are the flexibility price and the default flexibility offered by the upstream network. To assess the impact of essential flexibility parameters on the operational cost, Fig. 7 is incorporated. Using Fig. 7, it can be seen that an increase in flexibility defaults, while keeping flexibility prices constant, leads to a decrease in the

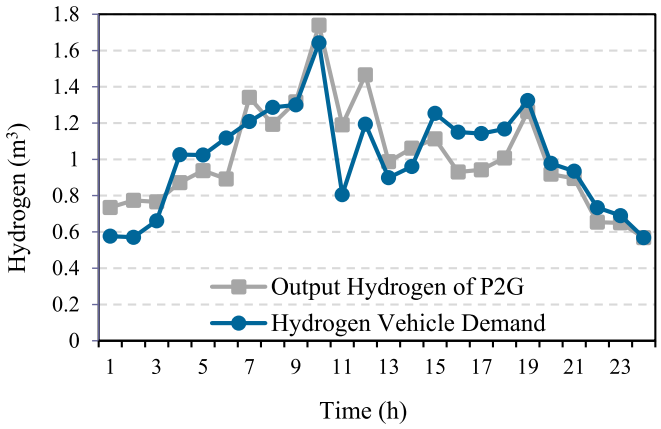


**Fig. 10.** The output hydrogen of the P2G unit and the demand for the HVs.

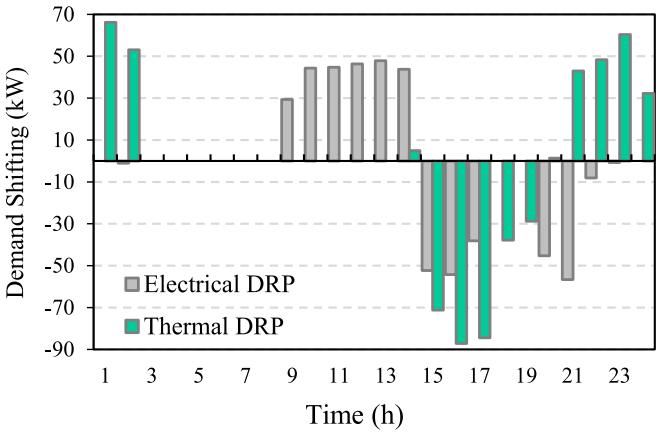


**Fig. 12.** The electrical and heat demand response programs.

operational cost of the LMCES. Nevertheless, the consequences on the operational cost of the LMCES, when increasing flexibility prices while keeping flexibility defaults constant, are contingent upon whether the flexibility default is low or high. In the case of low flexibility defaults, such as 0 kW, raising the flexibility price results in an increase in the operational cost as the LMCES cannot meet the system operator's specified flexibility default. However, for higher flexibility defaults, such as 50, 100, and 150 kW, the operational cost decreases as the flexibility prices increase. The optimal hourly flexibility for the LMCES is indicated in Fig. 8. It shows that increasing the flexibility price induces a heightened level of attention from the LMCES operator, leading to an enhancement in the overall operational flexibility of the upstream network.

The exchange of electrical, heat and gas energy with the upstream network is shown in Fig. 9. The findings reveal a consistent trend in the exchange of electrical energy with the upstream grid, primarily attributed to the consideration of flexibility constraint. Furthermore, the use of the PV system leads to a significant reduction in the procurement of electrical energy from the upstream network during sunny hours. Notably, the highest energy purchases occur in the time frame from 18 to 24, aligning with the period of heightened electrical load demand.

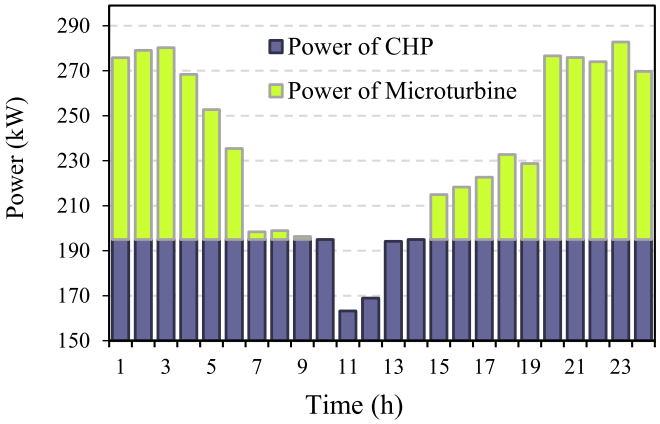


**Fig. 13.** The output power of the CHP and microturbine unit.

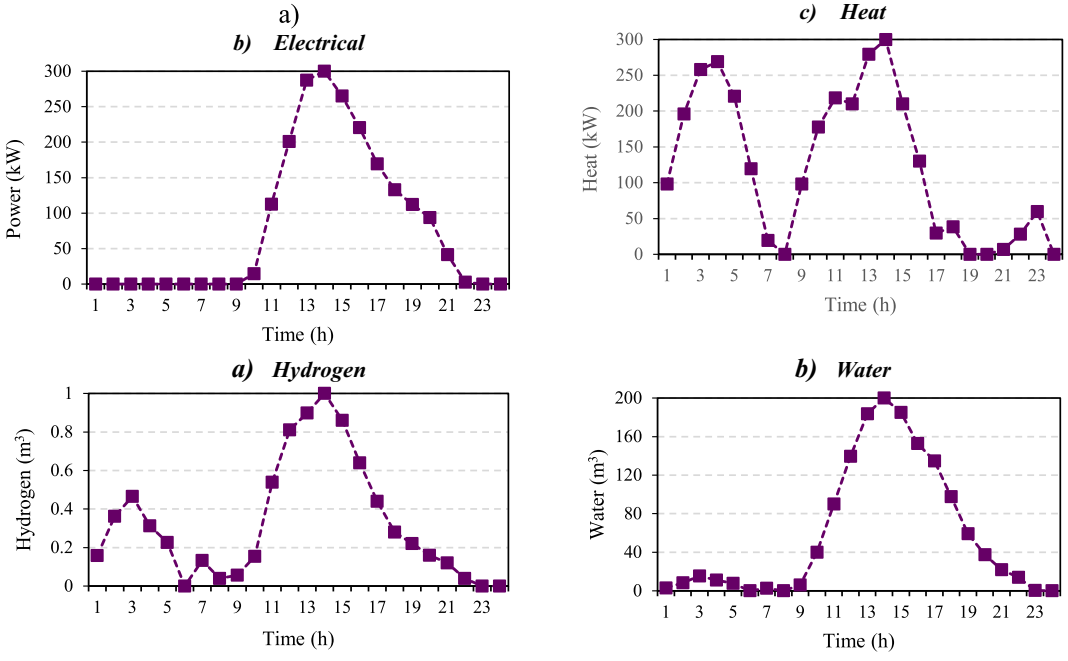


**Fig. 11.** The state of charge of storage systems: a) Electrical storage, b) Heat storage, c) Hydrogen storage, and d) Water storage.

Additionally, the results on heat energy exchange indicate that minimal procurement from the upstream network transpires during hours from 6 to 8, corresponding to peak heat prices and reduced heat demand. Moreover, key gas-consuming components in the proposed LMCES include boiler unit, CHP unit, microturbine, and gas demand, all of which collectively shape the level of natural gas procured from the upstream gas network. Taking into account the performance of the PV system, which generates power during midday hours, a simultaneous decrease is observed in the electricity output of both the microturbine and the CHP unit. Consequently, this decrement in electricity generation leads to a reduced dependence on natural gas acquisition from the upstream gas network during these specific time intervals.

The hydrogen production of the P2G unit and the demand of HVs are graphically depicted in Fig. 10. The P2G unit emerges as a pivotal and power-intensive component within the LMCES. This component synergistically interfaces with renewable energy systems, such as the PV system, to efficiently capture and store surplus energy in the form of hydrogen. The findings demonstrate the effective synchronization of hydrogen production by the P2G unit with the demand of HVs for a significant portion of the day. Notably, during sunny hours, the P2G unit generates an excess of hydrogen surpassing immediate demand, thereby offering potential for subsequent utilization through controlled hydrogen discharge later in the day.

The status of the electrical, heat, hydrogen, and water storage systems' charges is presented in Fig. 11. It can be concluded that the electrical storage unit undergoes charging between hours 10–14, aligning with sunny hours and off-peak demand periods. Furthermore, the electrical energy storage system is discharged during peak pricing periods. The operation of the heat energy storage system is primarily influenced by the upstream heat energy price, as it charges during hours 1–4 and 9–14, and discharges during hours 5–8 and 15–19. Additionally, the hydrogen storage system charges during sunny hours and reserves stored hydrogen for later use, thereby fulfilling the hydrogen demand of hybrid vehicles. The water storage unit is charged by the water desalination unit during the midday hours when the PV system generates power and electrical energy prices are low. Subsequently, it discharges during high electricity price hours, effectively reducing power consumption by the water desalination unit during peak pricing periods.

The findings of the electrical and heat DRP are shown in Fig. 12. It is evident that both programs exhibit remarkable efficacy in reducing demand during peak hours when energy prices are at their highest, while also adequately fulfilling demand during off-peak hours when energy prices are lower.

Fig. 13 depicts the power generation outputs of the CHP unit and the microturbine unit. Analysis of the results indicates that both units consistently operate at their maximum power outputs for the majority of the day. Nevertheless, during midday hours when the PV system generates substantial power and electricity prices are relatively low, the microturbine unit is deactivated, resulting in a decrease in power output from the CHP unit. Moreover, Fig. 14 illustrates the heat outputs of the boiler unit and the CHP unit. The heat generation from these units is carefully aligned with the heat requirement and heat energy pricing within the LMCES. This coordination ensures that the heat output is efficiently tailored to meet the heating and energy needs of the system, while also optimizing cost efficiencies relative to heat energy pricing.

The water output of the desalination unit is shown in Fig. 15. Analysis of the data indicates that the unit produces potable water during daylight hours and stores it in the water storage system. This approach plays a crucial role in mitigating the energy consumption of the

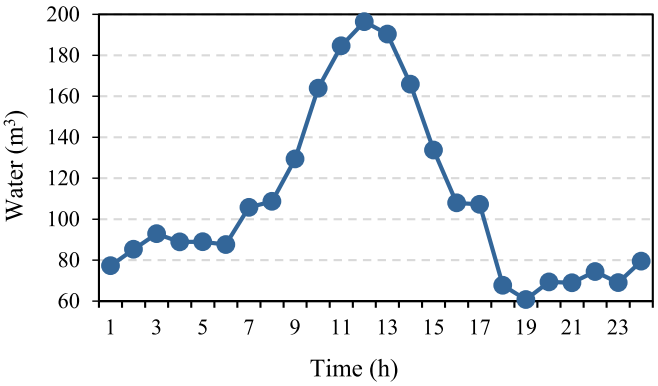


**Fig. 15.** The output water of the desalination unit.

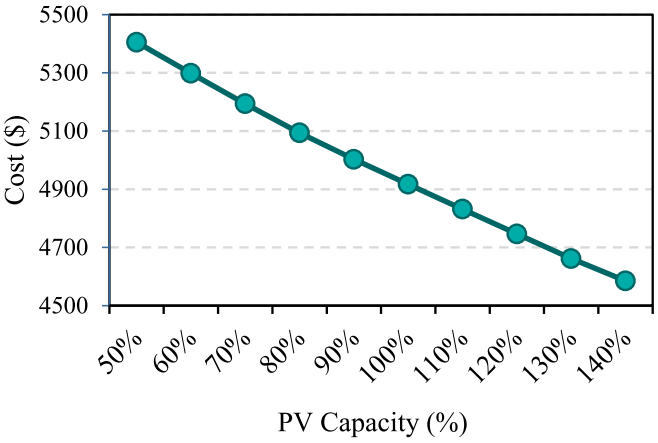


**Fig. 16.** The impact of PV system capacity on operation cost reduction.

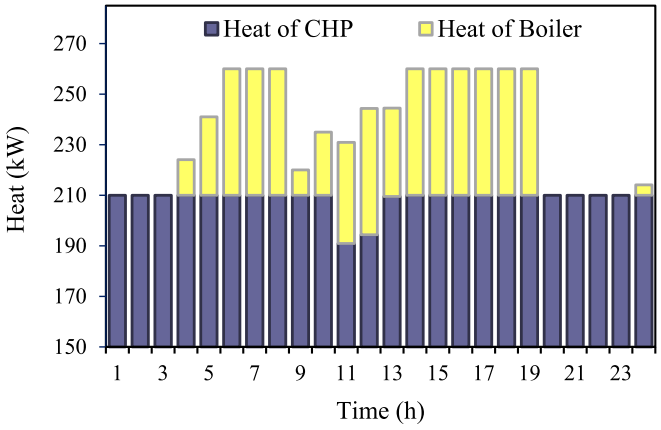


**Fig. 14.** The output heat of the boiler and CHP unit.

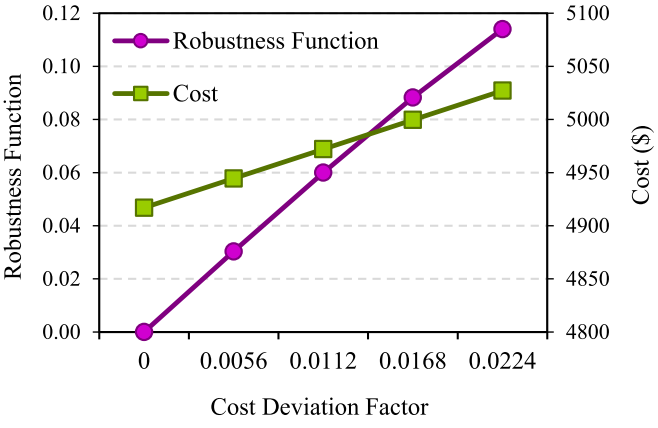


**Fig. 17.** The performance of the LMCES system in the risk-avares mode.

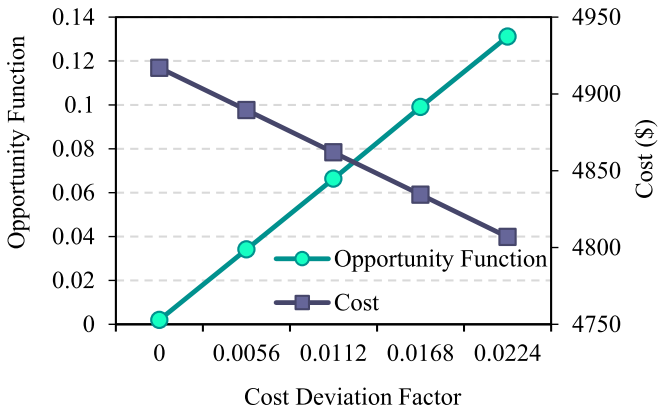


**Fig. 18.** The performance of the LMCES system in the risk-seeker mode.

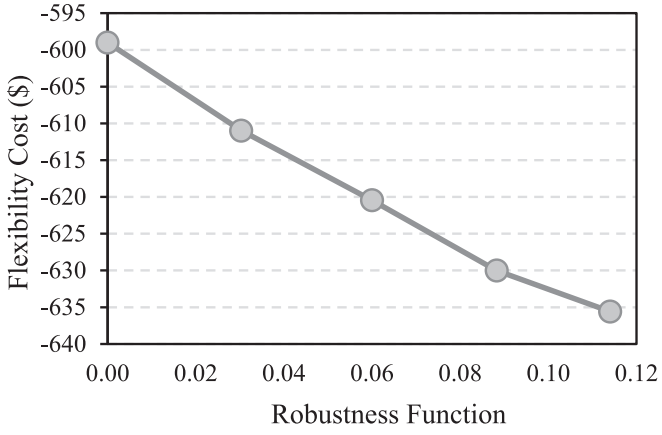


**Fig. 19.** The robustness function vs flexibility cost analysis in the risk-averse strategy.

desalination unit during subsequent periods.

Renewable energy resources, such as PV systems, play a significant role in reducing the costs associated with LMCES. To quantitatively evaluate this impact, Fig. 16 illustrates the correlation between PV system capacity and operational costs. The analysis shows that a 40 % increase in PV system capacity leads to a 6.74 % reduction in operational costs. This cost reduction is attributed to the increased availability of renewable energy, thereby diminishing the reliance on more costly conventional energy sources. Conversely, a 40 % decrease in PV system capacity results in a 7.75 % increase in operational costs. These findings underscore the importance of optimizing PV system capacity to achieve cost-effective and sustainable energy management within LMCES.

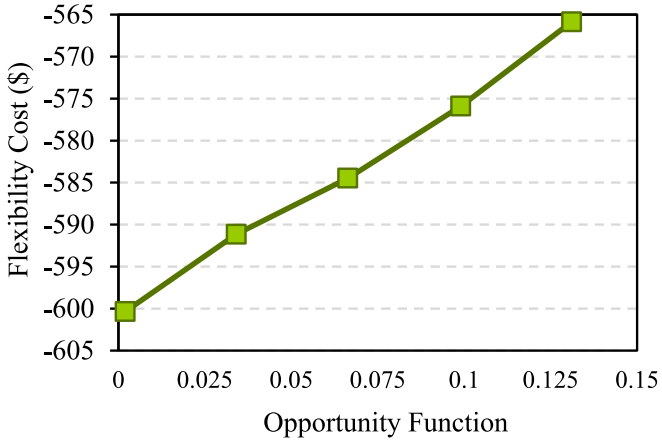


**Fig. 20.** The opportunity function vs flexibility cost analysis in the risk-seeker strategy.

#### 4.2.2. *Hybrid probabilistic-IGDT results*

In this section, the results of the hybrid Probabilistic-IGDT approach have been presented. Utilizing the previously determined no-risk cost of $4916.99, both risk-averse and risk-seeking analyses were conducted. By applying the proposed hybrid model to solve the scheduling problem for $\zeta = 0$ to $\zeta = 0.0224$, the optimum robustness and opportunity functions, as well as critical costs, have been identified, which are illustrated in Fig. 17 and Fig. 18, respectively. The analysis revealed that the impact of uncertainty within the PV system on the net cost appears to be negligible in the risk-averse mode. Even a discrepancy of 11 % in PV system forecasting results in only a 2.24 % rise in operational cost, highlighting the robustness of the proposed approach in risk-averse scenarios. Conversely, the opportunity function within the framework serves as a tool to quantify potential cost reductions or advantageous outcomes linked to various decision alternatives. The results indicate that the operation cost of the LMCES decreases in proportion to the optimism of the operator. However, it is important to note that this optimistic approach may prove challenging in situations where uncertainties are realized to a significant extent.

The impact of the LMCES owner's risk strategy on participation in the flexibility program is evaluated in Figs. 19 and 20, considering risk-averse and risk-seeking strategies, respectively. Fig. 19 demonstrates that the flexibility profit of the LMCES owner increases as the robustness function is enhanced. This is attributed to a reduction in PV system generation, leading to a decrease in the ramp rate of power exchange with the grid, thereby increasing the flexibility profit. On the other hand, Fig. 20 depicts the correlation between flexibility cost/profit and the opportunity function. It shows that as the opportunity function increases, indicating a risk-seeker strategy, PV system generation also increases. However, this results in a decline flexibility profit due to higher ramp rates and less effective participation in the flexibility program.

## 5. Conclusion

This research introduces a multi-objective optimization model designed specifically for the LMCES aiming at minimizing operation costs and reducing emissions. The model consists of two layers: the *physical layer*, which encompasses a multi-carrier energy system including electrical, heat, gas, and water infrastructure, as well as provisions for HVs and hydrogen refueling stations; and the managerial layer, which integrates a flexibility constraint to align with the LMCES's proactive approach to enhancing flexibility through optimization. Additionally, the model effectively addresses uncertainties associated with energy prices and demand using scenario-based methods. The results highlight the LMCES's ability to execute optimal flexibility-oriented optimization, emphasizing the pivotal influence of flexibility default and flexibility price on performance. Specifically, the flexibility price leads to a 3.07 % cost reduction in low flexibility default scenarios and a substantial 29.64 % reduction in high flexibility default scenarios. The findings underscore the delicate balance between minimizing emissions and operational costs, emphasizing the need for careful selection of optimal operating points from the Pareto frontier by LMCES operators. Notably, the collaborative operation of the P2G unit and the hydrogen storage system is identified as a crucial factor in cost reduction. An innovative aspect of this study is the consideration of hydrogen vehicle availability as a random parameter, suggesting that future research could explore the integration of HV owners within the LMCES, incorporating behavioral theories as a promising avenue for further investigation. In future research, there is a need for further exploration into demand response strategies, which could encompass the consideration of additional energy carriers such as water and gas loads.

Moreover, the investigation of the flexibility of heat energy holds promise as a research topic for future inquiries. Furthermore, it would be beneficial for future research to explore a bi-level framework to assess how the involvement of LMCES in flexibility programs affects the reserve capacity of the upstream power system.

## CRediT authorship contribution statement

**Sobhan Dorahaki:** Writing – original draft, Methodology, Investigation, Data curation. **Mojgan MollahassaniPour:** Writing – original draft, Methodology. **Masoud Rashidinejad:** Writing – review & editing, Validation, Supervision, Formal analysis, Conceptualization. **Pierluigi Siano:** Writing – review & editing, Visualization, Supervision. **Miadreza Shafie-khah:** Writing – review & editing, Validation, Funding acquisition, Formal analysis.

## Declaration of competing interest

The authors declare that they have no known competing financial interests or personal relationships that could have appeared to influence the work reported in this paper.

## Data availability

Data will be made available on request.

## Acknowledgement

This work of Pierluigi Siano was supported in part by the Ministry of Research, Innovation and Digitalization under Project PNRR-C9-I8-760090/23.05.2023 CF30/14.11.2022.

## Appendix A. Appendix

The participation of users in electric and heat load-shifting demand response is represented by Eqs. (A1)–(A10). The limits for electrical / heat upward and downward DRPs are defined by Eqs. (A1) and (A2) / (A6) and (A7), respectively; Eq. (A3) / Eq. (A8) ensures that the cumulative upward and downward electrical / heat demand response remains balanced; the simultaneous implementation of electrical / heat upward and downward demand response is constrained by Eq. (A4) / Eq. (A9); the electrical / heat demand after implementing electrical load shifting DRP is calculated using Eq. (A5) / Eq. (A10) [51]

$$0 \le \mu_{i,t,s}^{\mathrm{E,up}} \le \vartheta^{\mathrm{E}} I_{i,t,s}^{\mathrm{E,up}} EL_{i,t,s} \tag{A1}$$

$$0 \le \mu_{i,t,s}^{\mathrm{E,dn}} \le \vartheta^{\mathrm{E}} I_{i,t,s}^{\mathrm{E,dn}} EL_{i,t,s} \tag{A2}$$

$$\sum_{t=1}^{N_t} \mu_{i,t,s}^{\mathrm{E,up}} = \sum_{t=1}^{N_t} \mu_{i,t,s}^{\mathrm{E,dn}} \tag{A3}$$

$$I_{i,t,s}^{\mathrm{E,up}} + I_{i,t,s}^{\mathrm{E,dn}} \le 1 \tag{A4}$$

$$EL_{i,t,s}^{\mathrm{DR}} = EL_{i,t,s} + \mu_{i,t,s}^{\mathrm{E,up}} - \mu_{i,t,s}^{\mathrm{E,dn}} \tag{A5}$$

$$0 \le \mu_{f,t,s}^{\mathrm{T,up}} \le \vartheta^{\mathrm{T}} I_{f,t,s}^{\mathrm{T,up}} TL_{f,t,s} \tag{A6}$$

$$0 \le \mu_{f,t,s}^{\mathrm{T,dn}} \le \vartheta^{\mathrm{T}} I_{f,t,s}^{\mathrm{T,dn}} TL_{f,t,s} \tag{A7}$$

$$\sum_{t=1}^{N_t} \mu_{f,t,s}^{\mathrm{T,up}} = \sum_{t=1}^{N_t} \mu_{f,t,s}^{\mathrm{T,dn}} \tag{A8}$$

$$I_{f,t,s}^{\mathrm{T,up}} + I_{f,t,s}^{\mathrm{T,dn}} \le 1 \tag{A9}$$

$$TL_{f,t,s}^{\mathrm{DR}} = TL_{f,t,s} + \mu_{f,t,s}^{\mathrm{T,up}} - \mu_{f,t,s}^{\mathrm{T,dn}} \tag{A10}$$

## References

[1] Dorahaki S, Rashidinejad M, MollahassaniPour M, Pourakbari Kasmaei M, Afzali P. A sharing economy model for a sustainable community energy storage considering end-user comfort. Sustain Cities Soc Oct. 2023;97:104786. https://doi.org/10.1016/j.scs.2023.104786.

[2] Ahmed I, Alvi U-E-H, Basit A, Rehan M, Hong K-S. Multi-objective whale optimization approach for cost and emissions scheduling of thermal plants in energy hubs. Energy Rep Nov. 2022;8:9158–74. https://doi.org/10.1016/j.egyr.2022.07.015.

[3] Dorahaki S, Rashidinejad M, Fatemi Ardestani SF, Abdollahi A, Salehizadeh MR. An integrated model for citizen energy communities and renewable energy communities based on clean energy package: a two-stage risk-based approach. Energy Aug. 2023;277:127727. https://doi.org/10.1016/j.energy.2023.127727.

[4] Dorahaki S, Sarkhosh A, Rashidinejad M, Salehizadeh MR, MollahassaniPour M. Fairness in optimal operation of transactive smart networked modern multi-carrier energy systems: a two-stage optimization approach. Sustain Energy Technol Assessments Mar. 2023;56:103035. https://doi.org/10.1016/j.seta.2023.103035.

[5] Akbarizadeh M, Niknam T, Jokar H. Economic operation of networked flexi-renewable energy hubs with thermal and hydrogen storage systems based on the market clearing price model. Int J Hydrog Energy Jul. 2023. https://doi.org/10.1016/j.ijhydene.2023.06.144.

[6] IEA CO2 emissions from fuel combustion: Overview IEA, Paris (2020), https://www.iea.org/reports/co2-emissions-from-fuel-combustion-overview.

[7] Corsetti E, Riaz S, Riello M, Mancarella P. Modelling and deploying multi-energy flexibility: the energy lattice framework. Adv Appl Energy May 2021;2:100030. https://doi.org/10.1016/j.adapen.2021.100030.

[8] Rabiee A, Keane A, Soroudi A. Green hydrogen: a new flexibility source for security constrained scheduling of power systems with renewable energies. Int J Hydrog Energy 2021;46(37):19270–84. https://doi.org/10.1016/j.ijhydene.2021.03.080.

[9] Rahgozar S, Seyyedi A Zare Ghaleh, Siano P. A resilience-oriented planning of energy hub by considering demand response program and energy storage systems. J Energy Storage Aug. 2022;52:104841. https://doi.org/10.1016/j.est.2022.104841.

[10] Kashanizadeh B, Mohammadnezhad Shourkaei H, Fotuhi-Firuzabad M. A bi-stage multi-objectives optimization of smart multi energy system with active consumers. Sustain Prod Consum May 2022;31:707–22. https://doi.org/10.1016/j.spc.2022.03.028.

[11] Alabi TM, Agbajor FD, Yang Z, Lu L, Ogungbile AJ. Strategic potential of multi-energy system towards carbon neutrality: a forward-looking overview. Energy Built Environ Dec. 2023;4(6):689–708. https://doi.org/10.1016/j.enbenv.2022.06.007.

[12] Bahlawan H, Castorino GAM, Losi E, Manservigi L, Spina PR, Venturini M. Optimal management with demand response program for a multi-generation energy system. Energy Convers Manag X Dec. 2022;16:100311. https://doi.org/10.1016/j.ecmx.2022.100311.

[13] Wang J, Kang L, Liu Y. A multi-objective approach to determine time series aggregation strategies for optimal design of multi-energy systems. Energy Nov. 2022;258:124783. https://doi.org/10.1016/j.energy.2022.124783.

[14] Thang VV, Ha T, Li Q, Zhang Y. Stochastic optimization in multi-energy hub system operation considering solar energy resource and demand response. Int J Electr Power Energy Syst Oct. 2022;141:108132. https://doi.org/10.1016/j.ijepes.2022.108132.

[15] Mansouri SA, Nematbakhsh E, Ahmarinejad A, Jordehi AR, Javadi MS, Matin SAA. A multi-objective dynamic framework for design of energy hub by considering energy storage system, power-to-gas technology and integrated demand response program. J Energy Storage Jun. 2022;50:104206. https://doi.org/10.1016/j.est.2022.104206.

[16] Eladl AA, El-Afifi MI, Saeed MA, El-Saadawi MM. Optimal operation of energy hubs integrated with renewable energy sources and storage devices considering CO2 emissions. Int J Electr Power Energy Syst May 2020;117:105719. https://doi.org/10.1016/j.ijepes.2019.105719.

[17] Bahramara S. Robust optimization of the flexibility-constrained energy management problem for a smart home with rooftop photovoltaic and an energy storage. J Energy Storage Apr. 2021;36:102358. https://doi.org/10.1016/J.EST.2021.102358.

[18] Poorvaezi Roukerd S, Abdollahi A, Rashidinejad M. Probabilistic-possibilistic flexibility-based unit commitment with uncertain negawatt demand response resources considering Z-number method. Int J Electr Power Energy Syst Dec. 2019;113:71–89. https://doi.org/10.1016/j.ijepes.2019.05.011.

[19] Aghaei J, Bozorgavari SA, Pirouzi S, Farahmand H, Korpås M. Flexibility planning of distributed battery energy storage Systems in Smart Distribution Networks. Iran J Sci Technol Trans Electr Eng Sep. 2020;44(3):1105–21. https://doi.org/10.1007/s40998-019-00261-z.

[20] Pourghaderi N, Fotuhi-Firuzabad M, Moeini-Aghtaie M, Kabirifar M, Lehtonen M. Exploiting DERs' flexibility provision in distribution and transmission systems Interface. IEEE Trans Power Syst Mar. 2023;38(2):1963–77. https://doi.org/10.1109/TPWRS.2022.3209132.

[21] Hobbs BF, et al. Using probabilistic solar power forecasts to inform flexible ramp product procurement for the California ISO. Sol Energy Adv 2022;2:100024. https://doi.org/10.1016/j.seja.2022.100024.

[22] Poorvaezi Roukerd S, Abdollahi A, Rashidinejad M. Uncertainty-based unit commitment and construction in the presence of fast ramp units and energy storages as flexible resources considering enigmatic demand elasticity. J Energy Storage Jun. 2020;29:101290. https://doi.org/10.1016/j.est.2020.101290.

[23] Tang ZX, Lim YS, Morris S, Yi JL, Lyons PF, Taylor PC. A comprehensive work package for energy storage systems as a means of frequency regulation with increased penetration of photovoltaic systems. Int J Electr Power Energy Syst Sep. 2019;110:197–207. https://doi.org/10.1016/J.IJEPES.2019.03.002.

[24] Hamidpour H, Aghaei J, Dehghan S, Pirouzi S, Niknam T. Integrated resource expansion planning of wind integrated power systems considering demand response programmes. IET Renew Power Gener Mar. 2019;13(4):519–29. https://doi.org/10.1049/iet-rpg.2018.5835.

[25] Norouzi M, Aghaei J, Niknam T, Pirouzi S, Lehtonen M. Bi-level fuzzy stochastic-robust model for flexibility valorizing of renewable networked microgrids. Sustain Energy, Grids Networks Sep. 2022;31:100684. https://doi.org/10.1016/j.segan.2022.100684.

[26] Rinaldi A, Yilmaz S, Patel MK, Parra D. What adds more flexibility? An energy system analysis of storage, demand-side response, heating electrification, and distribution reinforcement. Renew Sust Energ Rev Oct. 2022;167:112696. https://doi.org/10.1016/j.rser.2022.112696.

[27] van Stiphout A, Brijs T, Belmans R, Deconinck G. Quantifying the importance of power system operation constraints in power system planning models: a case study for electricity storage. J Energy Storage Oct. 2017;13:344–58. https://doi.org/10.1016/j.est.2017.07.003.

[28] Després J, Mima S, Kitous A, Criqui P, Hadjsaid N, Noirot I. Storage as a flexibility option in power systems with high shares of variable renewable energy sources: a POLES-based analysis. Energy Econ May 2017;64:638–50. https://doi.org/10.1016/j.eneco.2016.03.006.

[29] Seward W, Qadrdan M, Jenkins N. Quantifying the value of distributed battery storage to the operation of a low carbon power system. Appl Energy Jan. 2022;305:117684. https://doi.org/10.1016/j.apenergy.2021.117684.

[30] Bozorgavari SA, Aghaei J, Pirouzi S, Nikoobakht A, Farahmand H, Korpås M. Robust planning of distributed battery energy storage systems in flexible smart distribution networks: a comprehensive study. Renew Sust Energ Rev May 2020;123:109739. https://doi.org/10.1016/j.rser.2020.109739.

[31] Chen S, Li Z, Li W. Integrating high share of renewable energy into power system using customer-sited energy storage. Renew Sust Energ Rev Jun. 2021;143:110893. https://doi.org/10.1016/j.rser.2021.110893.

[32] Ding Y, Shao C, Yan J, Song Y, Zhang C, Guo C. Economical flexibility options for integrating fluctuating wind energy in power systems: the case of China. Appl Energy Oct. 2018;228:426–36. https://doi.org/10.1016/j.apenergy.2018.06.066.

[33] Amaral Lopes R, Grønborg Junker R, Martins J, Murta-Pina J, Reynders G, Madsen H. Characterisation and use of energy flexibility in water pumping and storage systems. Appl Energy Nov. 2020;277:115587. https://doi.org/10.1016/j.apenergy.2020.115587.

[34] Pierro M, Perez R, Perez M, Moser D, Cornaro C. Imbalance mitigation strategy via flexible PV ancillary services: the Italian case study. Renew Energy Dec. 2021;179:1694–705. https://doi.org/10.1016/j.renene.2021.07.074.

[35] Agbonaye O, Keatley P, Huang Y, Odiase FO, Hewitt N. Value of demand flexibility for managing wind energy constraint and curtailment. Renew Energy May 2022;190:487–500. https://doi.org/10.1016/j.renene.2022.03.131.

[36] Zubo RHA, Mokryani G. Active distribution network operation: a market-based approach. IEEE Syst J Mar. 2020;14(1):1405–16. https://doi.org/10.1109/JSYST.2019.2927442.

[37] Jiang T, Wu C, Zhang R, Li X, Chen H, Li G. Flexibility clearing in joint energy and flexibility markets considering TSO-DSO coordination. IEEE Trans Smart Grid Mar. 2023;14(2):1376–87. https://doi.org/10.1109/TSG.2022.3153634.

[38] RaeisiNia MR, Javadi S, Jokar MR, Nejati SA. Flexibility pricing in the active distribution network including renewable and flexibility sources as a bi-level optimization model. Sustain Energy Technol Assessments Aug. 2022;52:101947. https://doi.org/10.1016/j.seta.2021.101947.

[39] Maroufmashat A, et al. Modeling and optimization of a network of energy hubs to improve economic and emission considerations. Energy Dec. 2015;93:2546–58. https://doi.org/10.1016/j.energy.2015.10.079.

[40] Soroudi A, Keane A. Risk Averse Energy Hub Management Considering Plug-in Electric Vehicles Using Information Gap Decision Theory. 2015. p. 107–27.

[41] Martinez-Mares A, Fuerte-Esquivel CR. A robust optimization approach for the interdependency analysis of integrated energy systems considering wind power uncertainty. IEEE Trans Power Syst Nov. 2013;28(4):3964–76. https://doi.org/10.1109/TPWRS.2013.2263256.

[42] Rastegar M, Fotuhi-Firuzabad M, Zareipour H, Moeini-Aghtaieh M. A probabilistic energy management scheme for renewable-based residential energy hubs. IEEE Trans Smart Grid Sep. 2017;8(5):2217–27. https://doi.org/10.1109/TSG.2016.2518920.

[43] Neyestani N, Yazdani-Damavandi M, Shafie-khah M, Chicco G, Catalao JPS. Stochastic modeling of multienergy carriers dependencies in smart local networks with distributed energy resources. IEEE Trans Smart Grid Jul. 2015;6(4):1748–62. https://doi.org/10.1109/TSG.2015.2423552.

[44] Chen S, Wei Z, Sun G, Cheung KW, Sun Y. Multi-linear probabilistic energy flow analysis of integrated electrical and natural-gas systems. IEEE Trans Power Syst May 2017;32(3):1970–9. https://doi.org/10.1109/TPWRS.2016.2597162.

[45] Tiwari S, Singh JG. Optimal energy management of multi-carrier networked energy hubs considering efficient integration of demand response and electrical vehicles: a cooperative energy management framework. J Energy Storage Jul. 2022;51:104479. https://doi.org/10.1016/j.est.2022.104479.

[46] Monemi Bidgoli M, et al. Robust scheduling of hydrogen based smart micro energy hub with integrated demand response. Energy 2020;20(4):114393. https://doi.org/10.1016/j.apenergy.2019.114195.

[47] Dini A, Pirouzi S, Norouzi M, Lehtonen M. Grid-connected energy hubs in the coordinated multi-energy management based on day-ahead market framework. Energy Dec. 2019;188:116055. https://doi.org/10.1016/J.ENERGY.2019.116055.

[48] Jalili M, Sedighizadeh M, Sheikhi Fini A. Optimal operation of the coastal energy hub considering seawater desalination and compressed air energy storage system. Therm Sci Eng Prog Oct. 2021;25. https://doi.org/10.1016/J.TSEP.2021.101020.

[49] Zhang X, Shahidehpour M, Alabdulwahab A, Abusorrah A. Optimal expansion planning of energy hub with multiple energy infrastructures. IEEE Trans Smart Grid Sep. 2015;6(5):2302–11. https://doi.org/10.1109/TSG.2015.2390640.

[50] Dorahaki S, Rashidinejad M, Ardestani SFF, Abdollahi A, Salehizadeh MR. Probabilistic/information gap decision theory-based bilevel optimal management for multi-carrier network by aggregating energy communities. IET Renew Power Gener Jan. 2023. https://doi.org/10.1049/rpg2.12685.

[51] Lu X, Li H, Zhou K, Yang S. Optimal load dispatch of energy hub considering uncertainties of renewable energy and demand response. Energy Jan. 2023;262:125564. https://doi.org/10.1016/j.energy.2022.125564.

[52] Dorahaki S, Abdollahi A, Rashidinejad M, Moghbeli M. The role of energy storage and demand response as energy democracy policies in the energy productivity of hybrid hub system considering social inconvenience cost. J Energy Storage 2021; vol. 33, no. April 2020:102022. https://doi.org/10.1016/j.est.2020.102022.

[53] Chakraborty S. TOPSIS and modified TOPSIS: a comparative analysis. Decis Anal J Mar. 2022;2:100021. https://doi.org/10.1016/j.dajour.2021.100021.